Cyprus University of Technology

杭州電子科技大学
HANGZHOU DIANZI UNIVERSITY

Master's thesis

Pedestrian Dead Reckoning (PDR) Using Smart-phone IMU Sensors and Wireless Technologies

YU LINGMING

Limassol, May 2024

MSc in Electronics Science and Technology

CYPRUS UNIVERSITY OF TECHNOLOGY

Faculty of Engineering and Technology

Department of Electrical Engineering, Computer Engineering, and Informatics

Master's thesis

Pedestrian Dead Reckoning (PDR) Using Smart-phone IMU Sensors and Wireless Technologies

YU LINGMING

Supervisor

Michalis Michaelides

Limassol, May 2024

Approval Form

Master's thesis

Pedestrian Dead Reckoning (PDR) Using Smart-phone IMU Sensors and Wireless Technologies

Presented by

YU LINGMING

Supervisor: Michalis Michaelides

Member of the committee: ZHOU ZHOU

Member of the committee: ZHEN RUI

Cyprus University of Technology
Limassol, May 2024

Copyrights

Acknowledgements

I would like to thank [...], for [...]

ABSTRACT

As people spend increasingly more time living and working in indoor environments, researching and developing efficient and precise indoor positioning technology not only presents enormous market potential but also holds significant practical value. Existing Pedestrian Dead Reckoning (PDR) algorithms typically assume that pedestrians and smartphones maintain a relatively static relationship; however, this assumption is often unrealistic, as the orientation of smartphones changes with the movement of pedestrians during walking. Addressing this issue, this research builds on the built-in inertial sensors of smartphones, aiming to utilize low-cost MEMS sensors to achieve accurate step counting and heading estimation without imposing constraints on smartphone orientation. Furthermore, the research incorporates wireless technology to correct the cumulative errors of inertial sensors, thereby achieving higher positioning accuracy.The main work done in this thesis is as follows:

This research examines extensively the three main components of PDR algorithms.

(1) With regard to the step detection methodology, this study employs a unique step counting technique that decomposes the measurement data from smartphone IMU sensors (accelerometer, linear accelerometer, gyroscope and magnetometer) into their respective three-axis (x, y, z) components, creating various combinations of sensors axes to identify the optimal configuration. This method achieves precise and stable step estimation even without constraining the smartphone's position, effectively addressing a significant limitation in conventional approaches.

(2)Regarding step length estimation methodology, this study implements the Weinberg non-linear step length estimation model after comprehensive consideration of computational cost and estimation accuracy. This model precisely calculates the step length parameters for each pedestrian step, effectively balancing algorithmic precision with computational efficiency.

(3)This research applies an improved pedestrian heading estimation method that significantly reduces smartphone orientation constraints. The approach analyzes frequency domain characteristics of accelerometer data to identify characteristic frequency patterns of the walking direction axis, projecting acceleration data onto the geographic coordinate system through coordinate transformation. By combining angle traversal with digital signal processing techniques, the method achieves reasonably accurate automatic identification of walking direction, deriving heading angles through integration calculations.This method maintains good precision levels across various common smartphone holding positions.

Experimental outcomes demonstrate that under posture-unconstrained conditions, the PDR algorithm proposed in this research achieved excellent positioning results across two common usage scenarios: pocket mode and reading mode. The PDR system exhibited average positioning errors of 1.94 meters in pocket mode and 2.51 meters in reading mode. Through integration with WiFi positioning technology, system localization precision was substantially enhanced, with average positioning errors decreasing to 1.21 meters in pocket mode and 1.59 meters in reading mode, representing an overall average positioning error reduction of approximately 37%, effectively addressing the cumulative error challenge inherent to PDR. The system demonstrated remarkable stability and consistency across different carrying configurations, validating the feasibility and effectiveness of this methodology for practical implementations.

Keywords: Pedestrian dead reckoning, indoor positioning, smart phone, inertial sensor, WIFI

TABLE OF CONTENTS

LIST OF TABLES

LIST OF FIGURES

LIST OF ABBREVIATIONS

VAR	Virtual Augmented Reality
ADHD	Attention Deficit-Hyperactivity Disorder
BMI	Body Mass Index

1 Introduction

1.1 Background and Motivation

With the rapid iterative development of modern technology, smart devices such as smartphones, wearable devices, and smart home systems have not only improved the convenience of daily life but also created a new era of human-computer interaction and service experience, significantly enhancing social productivity and living efficiency. Empirical research shows that modern individuals spend approximately 70% to 90% of their time in various indoor environments[1], encompassing residential spaces, workplaces, commercial centers, and transportation hubs. Against this background, Location-Based Services (LBS)[2] [3]have demonstrated increasing strategic value, not only optimizing travel efficiency through precise navigation but also enabling rapid positioning and rescue of trapped individuals in emergency situations such as natural disasters, providing crucial support for emergency management, asset tracking, and personalized services.

In open environments, the Global Positioning System has established its technological dominance, providing precise positioning functions for smart terminals in open areas through direct satellite signal transmission [4], forming the infrastructure foundation for numerous location-dependent applications. However, when application scenarios shift to indoor environments, GPS technology faces significant challenges: signal attenuation and multipath interference caused by building structures, interior furnishings, and electronic devices substantially reduce the accuracy and reliability of positioning systems.

To address indoor positioning challenges, researchers have developed various non-satellite technology solutions[5]. Wi-Fi positioning technology[6] utilizes access point signal strength indicators to evaluate user spatial position; Bluetooth Low Energy technology[7] achieves fine positioning through beacon deployment based on its energy efficiency advantages; ultrasonic technology[8] provides high-precision positioning solutions by calculating spatial distances through signal propagation time differences. Although each technological approach has its characteristics, they generally depend on professional hardware and infrastructure, which not only increases the economic threshold for system implementation but also limits the widespread adoption of these technologies.

With cost optimization and performance enhancement of inertial sensor technology, Pedestrian Dead Reckoning (PDR) has gradually become a research focus due to its unique advantages[9]. PDR technology derives pedestrian position and trajectory information[10] by analyzing sensor data during walking, combining gait recognition, step length calculation, and direction determination, providing a relatively autonomous technical path for indoor positioning. The array of sensors integrated in contemporary smartphones, including accelerometers, gyroscopes, and magnetometers[11], provides a solid hardware foundation for PDR technology implementation, capable of capturing real-time pedestrian dynamic information and providing necessary data support for precise position calculation.

with the popularity of smart phones[12],PDR technology based on built-in sensors of smart terminals not only meets daily indoor positioning needs but also has the potential to play a key role in diverse fields such as commercial activities and emergency rescue, holding significant practical importance for promoting social and economic development and enhancing the quality of public life.

1.2 Aims and Objectives

Aim:

This research aims to explore an adaptive pedestrian localization solution designed to improve system responsiveness to smartphone orientation changes and the diversity of user behaviors during movement. The research methodology combines complementary filtering with multi-source wireless technologies (such as Wi-Fi signal processing) to enhance positioning performance in complex, dynamic environments, although current research still focuses on two-dimensional positioning on a single plane. This study hopes to alleviate, to some extent, existing indoor positioning challenges related to device orientation limitations and positioning biases caused by pedestrian behaviors.

Objectives:

1.In the current research domain, the step detection component remains constrained by the spatial orientation of smart terminals, which to some extent impacts the practicality of positioning systems. Addressing this real-world challenge, this study focuses on exploring step detection methodologies with reduced posture sensitivity[13], aiming through technical improvements to maintain relatively reliable step counting capabilities under conditions where device positioning varies. This consideration of adaptability to natural usage scenarios more closely aligns with the actual requirements of users' unconscious operations in daily life, helping to narrow the gap between laboratory environments and practical applications.

2.Since the heading estimation module faces the most severe device posture constraints in traditional positioning methods, this research, through thoughtfully designed computational approaches, attempts to achieve effective alignment between smartphone coordinate frameworks and pedestrian movement characteristics. The algorithm aims to maintain positioning stability across different usage contexts—including handheld states, pocket carrying, and other common usage patterns—demonstrating good adaptability and enabling relatively accurate estimation of pedestrian heading while reducing dependence on device orientation that traditional positioning methods require. This provides a more flexible technical solution for practical application scenarios.

3.The research enhances system adaptability to complex pedestrian movement patterns through optimized technical solutions. For typical walking behaviors such as turning, the study analyzes characteristic change patterns exhibited in inertial sensor data during direction changes, developing corresponding signal processing strategies to more accurately identify pedestrian turning actions. Based on these feature recognition results, the system implements targeted algorithm adjustment mechanisms that effectively reduce potential trajectory deviations during turning processes, improving trajectory estimation stability in dynamic walking scenarios.

4.The research objective is to explore and design a framework that attempts to achieve reasonable pedestrian heading estimation and step detection across various smartphone carrying positions. For the heading estimation component, the study references the posture-independent pedestrian heading estimation algorithm proposed by Donghui Liu[14], and building upon this foundation, aims to combine unrestricted smartphone posture step detection and heading components to construct a comprehensive PDR positioning system that is not constrained by smartphone orientation.

5.Explore multi-source fusion strategies[15] to utilize WiFi signals for correcting cumulative errors caused by Pedestrian Dead Reckoning (PDR), thereby enhancing overall positioning accuracy

1.3 Contribution

This research is based on the step detection and counting method proposed by Constantina[16], which improves step count estimation through intelligent classification and integration of sensor degrees of freedom. The study employs sensor integration technology in an attempt to enhance the accuracy and efficiency of pedestrian step detection.

The research objective is to explore and design a framework that attempts to achieve reasonable pedestrian heading estimation across various smartphone carrying positions. For the heading estimation component, the study references the posture-independent pedestrian heading estimation algorithm proposed by Donghui Liu, and builds upon this foundation by identifying pedestrian turning actions through inertial sensor data and implementing specialized processing for turning scenarios to potentially improve positioning performance.

This framework aims to adapt to individual gait characteristics and demonstrate potential adaptability in complex scenarios, including turns, stationary periods, and multi-level navigation environments. The research also considers integrating wireless signals (such as Wi-Fi[17]) in an effort to provide viable pedestrian positioning solutions in complex and dynamic environments.

1.4 Structure of the Thesis

Chapter 1:

This chapter addresses the research topic, highlighting its practical significance within the field, and summarizes the main direction, research objectives, and expected outcomes of this study. The content outlines the technical challenges facing pedestrian positioning technologies, establishing the problem background for the methodological system proposed in subsequent sections. Through this opening portion, readers can understand the importance of improving existing pedestrian positioning methods at both application and theoretical levels.

Chapter 2:

This chapter systematically examines the current state of research in pedestrian positioning, focusing on key components including step recognition techniques, direction estimation methods, wireless positioning calibration technologies (such as Wi-Fi and Bluetooth Low Energy), and altitude measurement based on barometric sensing. Through in-depth discussion of existing research achievements, the content reveals several issues and challenges in current studies, providing academic foundations for the theoretical construction and technical approach selection of this research.

Chapter 3:

This chapter begins with an introduction and explanation of the theoretical foundations of indoor positioning. It then provides a detailed exposition of the research methodology employed in this thesis, encompassing the construction process of step detection, heading estimation, step length estimation, and multi-source data processing algorithms. The content discusses approaches for effectively integrating different types of sensing data (including inertial measurement units, wireless signal characteristics, and barometric altitude information), and explores technical concepts for comprehensive optimization using factor graph structures.

Chapter 4:

This chapter details the experimental construction process, including test environment arrangement, data collection protocols, and evaluation scenario design. The study presents performance test results of the proposed technical framework and analyzes the differences between this method and existing technologies across multiple metrics, including positioning accuracy, system stability, and environmental adaptability.

Chapter 5:

This chapter provides an in-depth analysis of the experimental data, exploring the favorable aspects of system performance, existing limitations, and potential application value. It outlines the limitations of the current research and proposes directions for future work, providing a foundation for subsequent research in three-dimensional pedestrian positioning.

2 Literature Review

This chapter provides a comprehensive summary and analysis of existing research on smartphone-based pedestrian dead reckoning (PDR), focusing on four critical modules: step detection, heading estimation, step length estimation, and integration of wireless technologies for error correction. Step detection identifies and counts pedestrian steps, leveraging variations in sensor signals for accuracy. Heading estimation determines walking direction relative to a global reference frame, incorporating magnetometers, gyroscopes, and advanced fusion algorithms to minimize drift and magnetic interference. Step length estimation translates detected steps into traveled distances, considering individual characteristics and gait variability. Finally, wireless technology integration—using methods like Wi-Fi, GPS, Bluetooth, and UWB—aims to correct trajectory drift caused by cumulative PDR errors. By analyzing relevant studies, this chapter highlights advancements, limitations, and gaps in current research.

1. Step Detection

Step detection is a fundamental module in PDR systems, responsible for identifying walking activities and counting steps. Common approaches include peak detection, zero-crossing detection, and frequency-domain analysis. These methods often involve trade-offs between detection accuracy, computational complexity, and noise resilience.

Literature Analysis:

Kang et al. [18] proposed a gyroscope-based frequency-domain method for step detection and counting, achieving an accuracy of 93.76% across various carrying modes. The method extracts frequencydomain features from gyroscope signals to achieve high-precision step detection. However, its reliance on gyroscope data limits its applicability to low-cost devices, and its robustness in complex environments remains insufficiently verified.

Lin and Pan[19] developed a gait recognition technique that enhances system adaptability to various device carrying methods through horizontal component decomposition of acceleration data. While this approach achieved certain progress in step detection accuracy, its algorithm design overly relies on manual parameter adjustments, resulting in limited generalization performance when facing different users.

A interference-resistant step identification algorithm was constructed by Gu et al.[20] utilizing multiple-constraint gait feature analysis. Their approach effectively reduced false detection rates and demonstrated considerable accuracy under relatively consistent walking patterns. The fixed threshold strategy they implemented, however, showed inadequate performance when confronted with diverse gaits or dynamic scenarios, resulting in insufficient system robustness.

A multi-phase processing structure integrating signal filtration and walking pattern scoring mechanisms was developed by Salvi et al.[21], aiming to enhance step recognition precision in complex environments. Their methodology demonstrated certain advantages when handling challenging activities like running or stair navigation, yet when confronted with significant variations in gait patterns, there remains room for performance enhancement.

An enhanced dead reckoning methodology for pedestrian tracking was introduced by Zhao et al.[22], which incorporated data smoothing techniques and dynamic adjustments of acceleration magnitude to strengthen the system's resistance to abrupt gait variations. Despite demonstrating considerable stability in experimental settings, the performance of this algorithm remains noticeably susceptible to intense device oscillations.

Identified Constraints:

- Accommodation of varied walking patterns: Current technologies demonstrate suboptimal performance when confronted with unconventional movement forms such as leaping or sudden halts.
- Resilience in kinetic settings: Studies regarding performance under highly dynamic conditions like sprinting or traversing irregular surfaces remain insufficient.
- Self-adjusting capabilities: Approaches utilizing static thresholds lack dynamic calibration mechanisms driven by machine learning principles.
- Impact of device placement: Various methods of device carriage (handheld versus pocket placement) substantially affect detection precision.

2. Heading Estimation

Heading estimation is used to determine the movement direction of pedestrians relative to a global reference system (typically magnetic north). Such methods generally rely on magnetometers, gyroscopes, and sensor fusion algorithms (such as Kalman filters) for implementation. However, technical challenges such as magnetic interference and cumulative drift still exist.

Literature Analysis:

In their smartphone MEMS-IMU pedestrian dead reckoning solution, Kuang et al.[23] implemented zero angular rate update (ZARU) and static heading update (SHU) technologies to address drift issues. Their approach effectively reduced heading drift under relatively stable conditions; however, its performance was constrained when operating in dynamic environments characterized by rapid rotational movements or irregular motion patterns.

Geng et al.[24] combined magnetometer and barometric sensor data with Kalman filtering techniques in their three-dimensional indoor localization system utilizing smartphones. Their methodology stabilized directional estimation and enhanced vertical positioning accuracy, performing particularly well in structured settings such as predefined stairwells. The approach's dependence on structured environmental data, however, restricted its adaptability when deployed in unstructured or dynamic contexts.

Wang et al.[25] integrated magnetic fingerprinting techniques with particle filtering in their magnetic-based indoor positioning system designed for smartphones. Their approach substantially reduced heading drift through utilization of pre-constructed magnetic field maps. Despite demonstrating notable effectiveness, the necessity for high-quality magnetic mapping presented implementation challenges when considering diverse or uncalibrated environmental settings.

Tian et al.[26] incorporated dynamic observation variance adjustment techniques in their pedestrian dead reckoning system utilizing smartphone MARG sensors to address magnetic interference issues. While this adjustment enhanced the system's resistance to magnetic disturbances, it demonstrated restricted adaptability when confronted with complex walking patterns or significant variations in movement.

Kang and Han[27] created the SmartPDR system, which utilized multimodal sensor integration and deep learning techniques to dynamically forecast heading variations in smartphone-based pedestrian navigation for indoor settings. Their approach enhanced system stability in complex environments; however, it was constrained by computational demands that limited its real-time application capabilities.

Identified Constraints

- Stability in kinetic settings: Abrupt directional changes and intense device movements diminish heading reliability.
- Reliance on unchanging surroundings: The majority of approaches depend on static magnetic conditions or predetermined mapping, restricting adaptability.
- Cross-modal data synthesis: Research combining inertial measurements with visual or wireless information remains insufficient.
- Processing efficiency: Integration and neural network methodologies impose significant computational requirements.

3. Step Length Estimation

The conversion of identified footsteps into traversed distances is accomplished through step length estimation, a fundamental component within PDR frameworks. Prevalent methodologies encompass parametric formulations (such as the Weinberg equation), estimators based on machine learning, and adaptive models tailored to specific users. The following section examines pertinent studies, evaluating their contributions and inherent limitations.

Literature Analysis:

Principal component analysis (PCA) was utilized by Vezočnik et al.[28] to extract key gait characteristics, facilitating the development of a lightweight step length estimation model compatible with various device carrying positions. While their methodology demonstrated adaptability, verification in complex terrain environments such as stairways remained insufficient, leaving the performance efficacy across diverse settings inadequately substantiated.

A context-sensitive three-dimensional indoor localization system founded on pedestrian dead reckoning was proposed by Khalili et al.[29]. Their system achieved step length estimation accuracy of 1.5 meters through the incorporation of gender-specific parameters and step frequency correlations. The system's dependence on demographic inputs, however, constrained its applicability in anonymous settings such as public spaces.

An enhanced algorithm for pedestrian dead reckoning featuring a three-phase constraint model and dynamic drift elimination techniques was introduced by Zhao et al.[22], reducing step length estimation errors to below 2%. Despite its high precision, the algorithm's requirement for manual parameter calibration limited its scalability and user-friendliness.

Particle filtering and map matching techniques within a multimodal data integration framework were employed by Zhao et al.[30] to address cumulative error issues in step length estimation. While demonstrating excellence in reducing accumulated errors, their approach's strong dependence on precise indoor mapping resulted in diminished adaptability in scenarios where maps were unavailable.

An optimized algorithm integrating step frequency with acceleration magnitude to construct an adaptive model for estimating step length was developed by Salvi et [21]. While their method performed adequately under normal conditions, significant precision deterioration occurred when encountering rapid walking pattern variations or dynamic environmental contexts.

Identified Constraints

- Complex movement pattern challenges: Current models struggle with adaptation to dynamic activities like running or climbing.
- Real-time adjustment capabilities: Few systems provide step length estimation adjustments in real-time for unfamiliar users or varied environments.
- Multimodal data utilization: Limited application of pressure sensors, barometric instruments, or visual information to enhance estimation accuracy.
- Dependency on parameter configuration: Manual calibration requirements impede scalability and user independence.

4. Integration of Wireless Technologies for Error Correction

Various wireless technologies including Wi-Fi, Bluetooth, and magnetic fingerprinting are frequently utilized to rectify the accumulating errors in PDR systems. These approaches rely on environmental characteristics (such as signal intensity or distinctive patterns) to constrain positional deviations. The following section examines recent research contributions and their inherent limitations.

Literature Analysis:

GPS signals detected near windows were employed as indoor reference points for trajectory adjustment in the GPS-enhanced pedestrian navigation approach developed by Zhou and Maekawa[31]. Their methodology achieved notable accuracy in locations with GPS signal availability; however, it proved ineffective in providing dependable positioning within completely enclosed indoor spaces where GPS reception was absent.

Machine learning techniques were employed by Chandra[32] to combine Wi-Fi signal strength indicators with magnetic field measurements for enhanced indoor location estimation. Despite achieving significant precision, the method's reliability depended on the presence of multiple Wi-Fi access points, restricting its scalability in settings characterized by limited Wi-Fi coverage.

A dual-level integration mechanism combining extended Kalman filtering (EKF) with particle filtering (PF) was implemented by Wang et al.[25] in their magnetic-based indoor positioning framework. Their approach substantially improved localization accuracy through utilization of high-quality magnetic mapping. The system's reliance on such maps, however, presented implementation difficulties in environments without pre-established magnetic field data.

Multimodal data integration for three-dimensional indoor pedestrian positioning was accomplished by Zhao et al.[30] through the application of particle filtering techniques and barometric sensors. Their methodology effectively minimized cumulative positioning errors but demonstrated inadequate performance in dynamic situations where environmental factors, such as sudden movement alterations, compromised sensor data reliability.

A method for dynamically modifying magnetic pattern matching weights to accommodate signal variations in magnetic-based indoor positioning systems was introduced by Ashraf et al.[33]. Their dynamic weighting approach enhanced system adaptability to diverse signal conditions; however, performance deterioration was observed in highly obstructed settings characterized by significant magnetic interference.

Identified Constraints:

- Reliance on established infrastructure: Significant dependence on predetermined mapping or costly infrastructure restricts scalability.
- Vulnerability to signal fluctuations: Positional correction accuracy is affected by signal variations resulting from obstructions or interference.
- Scarcity of economical alternatives: Research concerning cost-effective techniques independent of mapping remains insufficient.
- Underutilized multiple data source integration: Investigation into the collaborative application of diverse wireless signals (including Wi-Fi, GPS, Bluetooth, and UWB) for positional adjustment requires further exploration.

5.Summary

Principal challenges present in current functional components of PDR:

1. Step detection: Insufficient adaptability to non-standard walking patterns and dynamic environmental contexts.
2. Heading estimation: Limited stability in kinetic environments and reliance on static surroundings.
3. Step length estimation: Inadequate real-time adjustment capabilities for varying users and movement patterns.
4. Wireless correction: High infrastructure dependency and deficient processing of dynamic signal variations.

Upcoming research endeavors should emphasize the utilization of artificial intelligence techniques, cross-sensor data integration, and self-adjusting computational methods to strengthen the modularity and resilience of pedestrian dead reckoning frameworks, facilitating their implementation across a wider spectrum of practical applications.

3 Research Methodology

3.1 Relevant theoretical basis

3.1.1 Introduction to Coordinate System

The geographic coordinate system represents a fundamental reference framework for determining positions on Earth's surface, utilizing longitude λ and latitude φ angles as key parameters. This system establishes its origin at Earth's center, with the Z-axis directed toward the North Pole, the X-axis pointing to the intersection of the Prime Meridian and Equator, while the Y-axis follows the right-hand rule to complete this three-dimensional reference frame. Geographic coordinates serve as the essential foundation for global positioning, navigation control, and geospatial information processing applications.

The local ENU (East-North-Up) coordinate system establishes a tangent plane reference frame at a specific point on Earth's surface, providing intuitive directional measurements for localized applications. East represents the perpendicular direction to the meridian plane pointing eastward, North aligns with the tangent to the meridian curve northward, and Up extends along the ellipsoidal normal. This localized framework enables precise relative positioning essential for navigation, surveying, and regional mapping where Earth's curvature effects must be minimized.

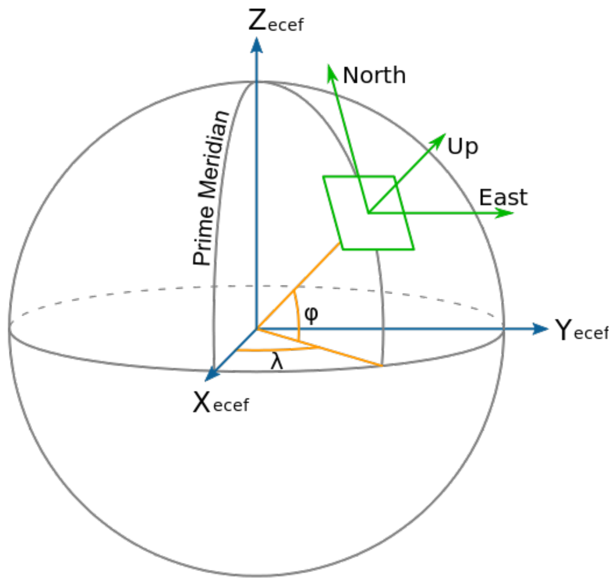

Figure 3.1: geographic coordinate system

The carrier coordinate system is a local coordinate system that moves with the carrier itself, with its origin typically set at the center of mass of the carrier, such as aircraft, ships, pedestrians, or smartphones. As shown in Figure 3.2, using a smartphone as an example, when the phone's screen faces upward, the y-axis of the b system is parallel to the phone screen and points forward, the x-axis is perpendicular to the y-axis and points to the right side of the phone screen, and the z-axis is perpendicular to both the x-axis and y-axis, pointing upward from the phone screen. This coordinate system setup is particularly suitable for analyzing and processing dynamic information related to the carrier, such as velocity, direction, and orientation, providing a necessary reference framework for precise control and navigation.

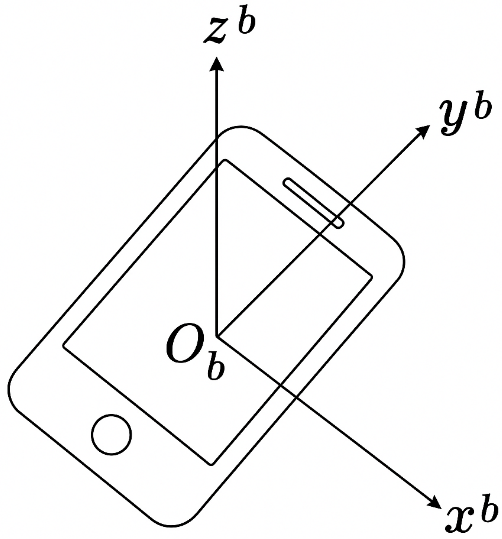

Figure 3.2: Carrier coordinate system

The navigation coordinate system, commonly referred to as the n-system, establishes a three-dimensional spatial framework with its origin at the center of mass of the pedestrian or carrier, related to the tangent plane of the Earth's surface. When studying indoor navigation problems, particularly in scenarios involving rapid positioning, we typically assume the carrier exists in a local environment unaffected by Earth's rotation and revolution effects. Consequently, the navigation coordinate system is simplified to match the geographic coordinate system's East-North-Up configuration. This arrangement not only complies with the right-hand rule but also provides a stable and intuitive reference for pedestrian movement within limited indoor spaces.

3.1.2 Introduction of Coordinate Transformation

Euler angles and rotation matrices

In three-dimensional space, any rigid body's attitude transformation can be achieved through rotations around three mutually perpendicular coordinate axes. This sequence of rotations and collection of angles, known as Euler angles, represents one method for describing object rotations in three-dimensional space [37]. Euler angles comprise three components: Pitch (denoted as θ), Roll (denoted as γ), and Yaw (denoted as ψ). For a smartphone's body coordinate system (b-frame), pitch represents the angle θ between the y-axis and the horizontal plane after rotation around the x-axis, roll represents the angle γ between the x-axis and the horizontal plane after rotation around the y-axis, and yaw represents the angle ψ between the projection of the y-axis on the horizontal plane and true north after rotation around the z-axis. Each Euler angle rotation can be represented by a rotation matrix, while the overall rotational state of an object can be obtained by multiplying these individual rotation matrices according to the rotation sequence. As shown in Figure 3.3, if the axes rotate according to the Z-Y-X Euler angle sequence, the specific process is as follows:

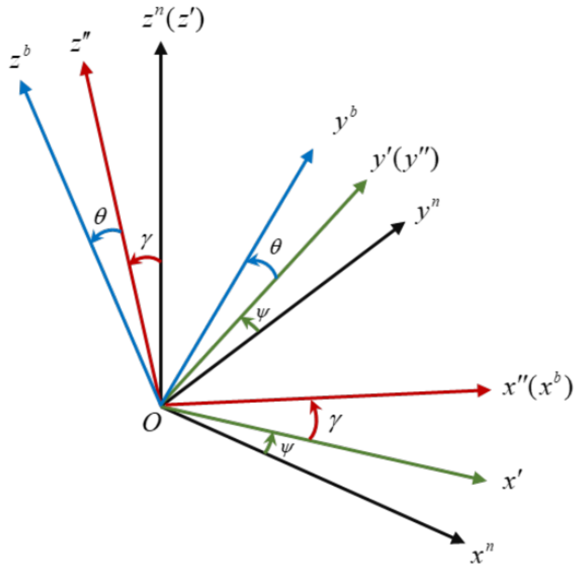

Figure 3.3: The transformation process from the navigation system to the carrier system coordinate system

First, the navigation coordinate system $O - x^n y^n z^n$ (or n-frame) is rotated by ψ degrees around the z^n axis to transform to the coordinate system $O - x'y'z'$, with the rotation matrix $R_z(\psi)$ as:

$$R_z(\psi) = \begin{bmatrix} \cos\psi & -\sin\psi & 0 \\ \sin\psi & \cos\psi & 0 \\ 0 & 0 & 1 \end{bmatrix} \tag{3.1}$$

Next, the coordinate system $O - x'y'z'$ is rotated by γ degrees around the y' axis to transform to the coordinate system $O - x''y''z''$, with the rotation matrix $R_y(\gamma)$ as:

$$R_y(\gamma) = \begin{bmatrix} \cos\gamma & 0 & \sin\gamma \\ 0 & 1 & 0 \\ -\sin\gamma & 0 & \cos\gamma \end{bmatrix} \tag{3.2}$$

Finally, the coordinate system $O - x''y''z''$ is rotated by θ degrees around the x'' axis to transform to the navigation coordinate system $O - x^b y^b z^b$, with the rotation matrix $R_x(\theta)$ as:

$$R_x(\theta) = \begin{bmatrix} 1 & 0 & 0 \\ 0 & \cos\theta & -\sin\theta \\ 0 & \sin\theta & \cos\theta \end{bmatrix} \tag{3.3}$$

The direction cosine matrix C_n^b of the b-frame relative to the n-frame is expressed as:

$$
\begin{aligned}
C_n^b &= R_z(\psi)R_y(\gamma)R_x(\theta) \\
&= \begin{bmatrix} \cos\psi & -\sin\psi & 0 \\ \sin\psi & \cos\psi & 0 \\ 0 & 0 & 1 \end{bmatrix} \begin{bmatrix} \cos\gamma & 0 & \sin\gamma \\ 0 & 1 & 0 \\ -\sin\gamma & 0 & \cos\gamma \end{bmatrix} \begin{bmatrix} 1 & 0 & 0 \\ 0 & \cos\theta & -\sin\theta \\ 0 & \sin\theta & \cos\theta \end{bmatrix}
\end{aligned} \tag{3.4}
$$

The rotation matrix defines the rotation of one coordinate system relative to another, conforming to the properties of orthogonal matrices. Therefore, the inverse operation of the rotation matrix, i.e., the inverse rotation, can be achieved by transposing the rotation matrix. Thus, the direction cosine matrix C_b^n of the n-frame relative to the b-frame is:

$$
C_n^b = (C_b^n)^T = \begin{bmatrix} \cos\gamma\cos\psi & \cos\gamma\sin\psi & -\sin\gamma \\ \sin\theta\sin\gamma\cos\psi - \cos\theta\sin\psi & \sin\theta\sin\gamma\sin\psi + \cos\theta\cos\psi & \sin\theta\cos\gamma \\ \cos\theta\sin\gamma\cos\psi + \sin\theta\sin\psi & \cos\theta\sin\gamma\sin\psi - \sin\theta\cos\psi & \cos\theta\cos\gamma \end{bmatrix} \tag{3.5}
$$

Quaternion method

Quaternions are mathematical tools[34] for representing three-dimensional rotations, consisting of one real and three imaginary parts (w,x,y,z). In navigation orientation, quaternions avoid the gimbal lock problem that affects Euler angles, offering computational efficiency and numerical stability, making them ideal for representing object orientation and performing smooth rotations in aerospace and robotics applications.The general form of quaternions can be expressed as:

$$
q = w + x\mathbf{i} + y\mathbf{j} + z\mathbf{k} \tag{3.6}
$$

Quaternions can be used to represent the rotation matrix of coordinate systems. The rotation matrix C_n^b from the n-frame to the b-frame shown in equation (3.4) can be expressed using quaternions as:

$$
C_b^n = \begin{bmatrix} 1 - 2q_2^2 - 2q_3^2 & 2(q_1q_2 - q_0q_3) & 2(q_1q_3 + q_0q_2) \\ 2(q_1q_2 + q_0q_3) & 1 - 2q_1^2 - 2q_3^2 & 2(q_2q_3 - q_0q_1) \\ 2(q_1q_3 - q_0q_2) & 2(q_2q_3 + q_0q_1) & 1 - 2q_1^2 - 2q_2^2 \end{bmatrix} \tag{3.7}
$$

The form of a quaternion expressed by Euler angles is as follows As shown below:

$$
\begin{bmatrix} q_0 \\ q_1 \\ q_2 \\ q_3 \end{bmatrix} = \begin{bmatrix} \cos\frac{\theta}{2}\cos\frac{\gamma}{2}\cos\frac{\psi}{2} + \sin\frac{\theta}{2}\sin\frac{\gamma}{2}\sin\frac{\psi}{2} \\ \sin\frac{\theta}{2}\cos\frac{\gamma}{2}\cos\frac{\psi}{2} - \cos\frac{\theta}{2}\sin\frac{\gamma}{2}\sin\frac{\psi}{2} \\ \cos\frac{\theta}{2}\sin\frac{\gamma}{2}\cos\frac{\psi}{2} + \sin\frac{\theta}{2}\cos\frac{\gamma}{2}\sin\frac{\psi}{2} \\ \cos\frac{\theta}{2}\cos\frac{\gamma}{2}\sin\frac{\psi}{2} - \sin\frac{\theta}{2}\sin\frac{\gamma}{2}\cos\frac{\psi}{2} \end{bmatrix} \tag{3.8}
$$

The conversion formula for converting quaternions to Euler angles is as follows:

$$\begin{bmatrix} \theta \\ \gamma \\ \psi \end{bmatrix} = \begin{bmatrix} \arctan \frac{2(q_0q_1+q_2q_3)}{1-2(q_1^2+q_2^2)} \\ \arcsin(2(q_0q_2 - q_1q_3)) \\ \arctan \frac{2(q_0q_3+q_1q_2)}{1-2(q_2^2+q_3^2)} \end{bmatrix} \tag{3.9}$$

3.1.3 Attitude update method based on quaternions

The current orientation of the smartphone is represented by quaternions, which, combined with real-time measurement data from the gyroscope sensor, enables real-time updates of the smartphone's attitude angles[35].

The differential equation of a quaternion describes the variation of a quaternion over time. The calculation formula of its differential equation is:

$$\dot{q} = \frac{1}{2} q \otimes \omega^b \tag{3.10}$$

where $\omega^b = \begin{bmatrix} 0 & \omega_x^b & \omega_y^b & \omega_z^b \end{bmatrix}^T$ is a pure quaternion with zero real part derived from the angular velocity measured by the gyroscope in the b-frame. the above expression can be transformed to:

$$\dot{q} = \frac{1}{2} \begin{bmatrix} q_0 & -q_1 & -q_2 & -q_3 \\ q_1 & q_0 & -q_3 & q_2 \\ q_2 & q_3 & q_0 & -q_1 \\ q_3 & -q_2 & q_1 & q_0 \end{bmatrix} \begin{bmatrix} 0 \\ \omega_x^b \\ \omega_y^b \\ \omega_z^b \end{bmatrix} \tag{3.11}$$

Since the gyroscope sensor samples at equal time intervals Δt, and the angular velocity changes between adjacent sampling periods are typically very small, by using Taylor expansion and retaining the first-order term, the quaternion update equation can be approximated as:

$$q_k \approx q_{k-1} + \frac{1}{2} \Delta t \cdot \dot{q}_{k-1} \tag{3.12}$$

where, q_{k-1} is the quaternion at time step $k-1$. Substituting equation (3.11) into the above expression yields:

$$q_k = \begin{bmatrix} q_0 \\ q_1 \\ q_2 \\ q_3 \end{bmatrix} + \frac{1}{2} \Delta t \begin{bmatrix} (-q_1\omega_x - q_2\omega_y - q_3\omega_z) \\ (q_0\omega_x + q_2\omega_z - q_3\omega_y) \\ (q_0\omega_y - q_1\omega_z + q_3\omega_x) \\ (q_0\omega_z + q_1\omega_y - q_2\omega_x) \end{bmatrix} \tag{3.13}$$

After each iteration, it should be ensured that the quaternions remain normalized, and the quaternions need to be normalized:

$$q = \frac{q}{\sqrt{(q_0^2 + q_1^2 + q_2^2 + q_3^2)}} \tag{3.14}$$

3.1.4 The basic principle of pedestrian navigation position calculation

”The PDR algorithm includes three components: step frequency detection, step length estimation, and heading estimation [36]. Smartphone-based PDR technology primarily utilizes the built-in accelerometer, magnetometer, and gyroscope to acquire pedestrian gait characteristic information, estimating the pedestrian’s step frequency, step length, and forward heading through data analysis and processing, and calculating the current position based on the position at the previous moment. The basic principle of PDR is shown in Figure 3.4. Assuming that a pedestrian’s position at a certain initial moment is known, their position during subsequent time periods can be calculated using formula (3.15).”

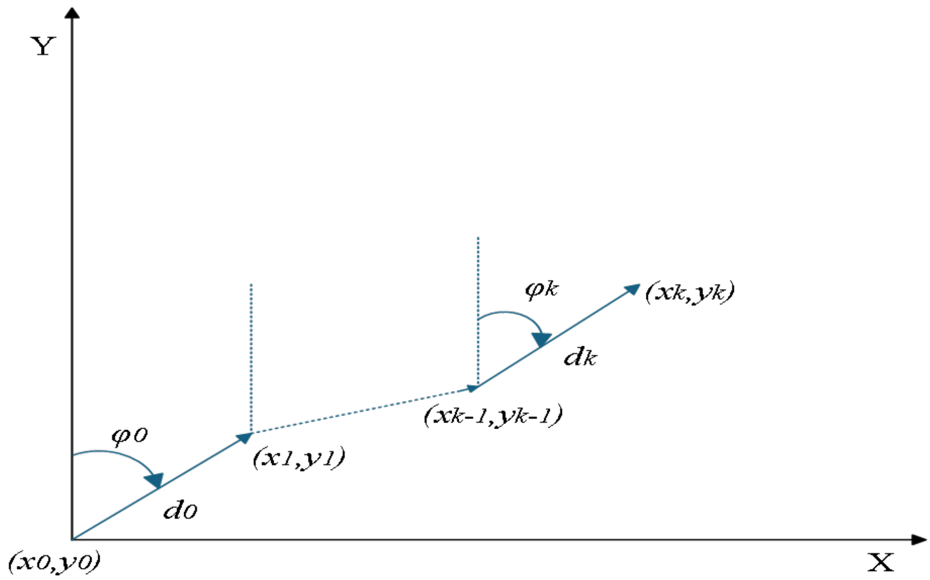

Figure 3.4: PDR (Pedestrian Dead Reckoning) Positioning

$$\begin{cases} x_k = x_{k-1} + d_{k-1} \sin \varphi_{k-1} \\ y_k = y_{k-1} + d_{k-1} \cos \varphi_{k-1} \end{cases} \tag{3.15}$$

3.2 Research Methodology Framework

This investigation examines a Pedestrian Dead Reckoning (PDR) system that functions without smartphone posture constraints. Figure 3.5 illustrates the comprehensive framework of the research methodology. Initially, raw data is collected through the smartphone’s built-in IMU sensors (accelerometer, gyroscope, magnetometer) and WiFi signals. The research conducts experiments using two representative smartphone carrying modes: pocket mode and reading mode, to evaluate the algorithm’s adaptability across different usage scenarios.

The PDR algorithm’s foundation comprises three essential modules: step detection, step length estimation, and heading estimation. The step detection module employs multi-sensor axis fusion techniques to achieve precise identification of pedestrian step frequency; the step length estimation module is based on an enhanced Weinberg non-linear model, calculating step length by considering pedestrian height and dynamic characteristics; the heading estimation module utilizes a posture-constraint-free algorithm, identifying walking direction through frequency domain analysis to enable reliable heading determination across various smartphone carrying methods.

The output information from these three modules undergoes integrated processing to generate PDR trajectories. To address the cumulative error issue in PDR systems, this study incorporates WiFi positioning technology, implementing a complementary filter to merge PDR and WiFi location information, effectively improving positioning accuracy. Finally, the system performance undergoes comprehensive evaluation and comparative analysis through a series of assessment metrics. Through this research framework, this study aims to reduce traditional PDR algorithms' dependence on smartphone posture, exploring a method that maintains satisfactory positioning accuracy across different smartphone carrying modes, providing a more flexible indoor positioning solution for everyday usage scenarios.

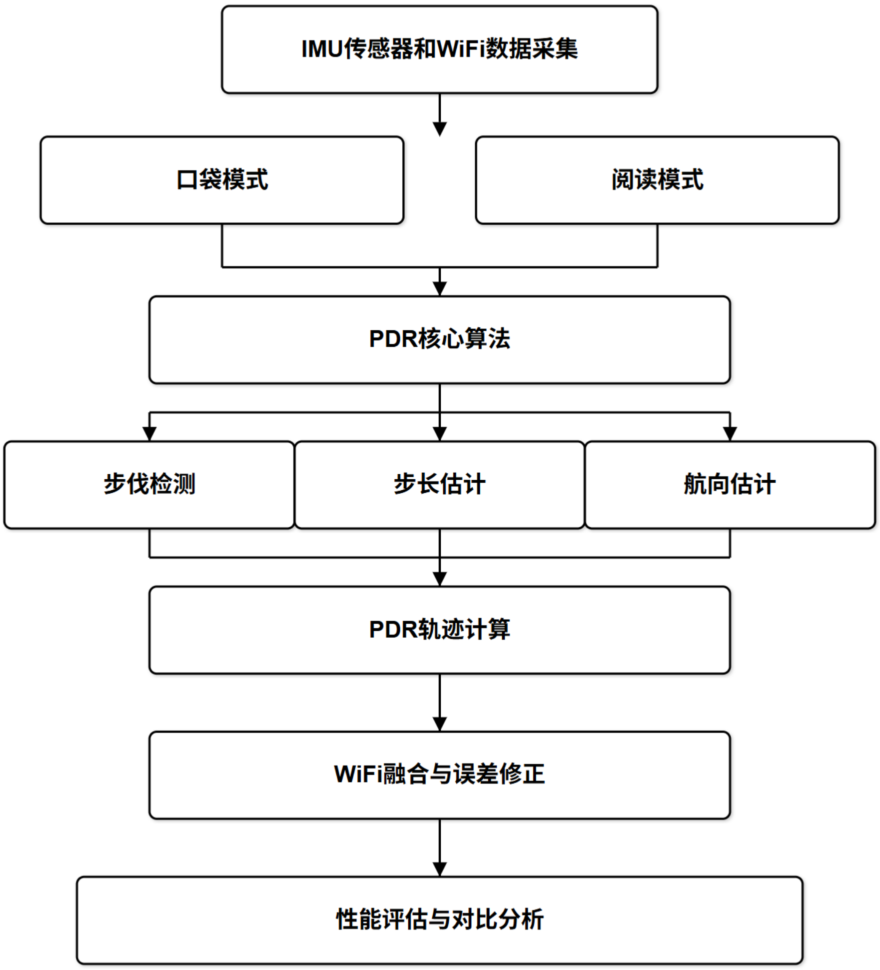

Figure 3.5: Flowchart of Research methods

3.3 The research method of Step detection used

3.3.1 Overview

This research implements the step detection methodology proposed by Isaia[16], which leverages multi-sensor axis fusion technology. Compared with conventional step length detection algorithms, this approach overcomes the limitations associated with single-sensor dependency by isolating and reconfiguring axis-specific data from various IMU sensors, thereby achieving enhanced gait recognition accuracy. In this chapter, we focus on elucidating the fundamental principles and technical characteristics of this methodology.

As a critical component of pedestrian dead reckoning systems, step detection accuracy directly affects overall positioning performance. Conventional methods typically rely on composite data from a single sensor (such as an accelerometer) to perform peak detection, often overlooking the rich information embedded in each axis component. The method adopted in this study is based on an innovative concept: treating the axis data from each sensor in smart devices—including accelerometers, linear accelerometers, gyroscopes, and magnetometers—as independent sources of information. By intelligently selecting and optimally combining these data, the accuracy and robustness of step detection are significantly enhanced. This approach not only addresses the limitations of single-sensor solutions but also adapts to variations in device placement and user walking patterns.

The flowchart of the step detection algorithm is as follows:

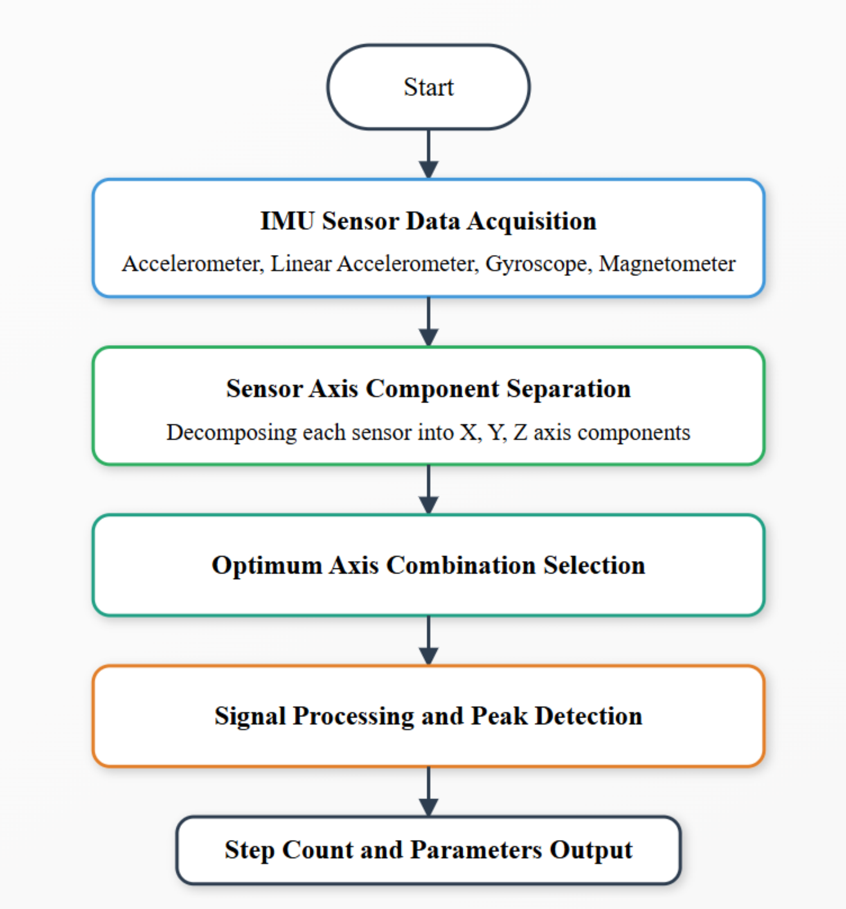

Figure 3.6: Flowchart of step detection algorithm

3.3.2 Theoretical basis

3.3.2.1 Signal Characteristic Analysis:

During human walking, complex motion patterns occur in multiple directions, which are captured by IMU sensors in different ways. Traditionally, the motion intensity is expressed as the composite magnitude of three-axis accelerations:

$$M_{\text{acc}}(t) = \sqrt{a_x^2(t) + a_y^2(t) + a_z^2(t)}$$

However, this composite approach has two major drawbacks: (1) Motion features along specific axes may be diminished after fusion, leading to the loss of distinctive directional characteristics; (2) Relying solely on acceleration makes it difficult to fully capture body rotation and directional changes during walking.

Biomechanical studies of human gait have identified key periodic characteristics of steps: when the foot strikes the ground, the vertical axis (typically the Z-axis) exhibits a distinct impact signal, appearing as a sharp peak in the acceleration magnitude. During the leg-swing phase, the body's center of gravity shifts posteriorly (usually along the Y-axis), while lateral sway mainly appears as periodic changes along the lateral axis (X-axis). Additionally, the body undergoes subtle rotations during walking, which are primarily captured as angular velocity variations by the gyroscope. Directional changes in walking are reflected in shifts in the geomagnetic field and are recorded by the magnetometer.

These multidimensional motion features tend to be averaged out or lost when relying on composite signals from a single sensor, which leads to information degradation. For instance, prominent vertical impact signals may be misinterpreted as noise in the horizontal direction, while body rotation features detected by the gyroscope are often overlooked in traditional methods. It is precisely these neglected dimensions of information that provide the theoretical foundation for multi-sensor axis fusion techniques.

3.3.2.2 Sensor signal separation and spatial expansion:

The first key component of this method lies in transforming fused sensor data into independent axis-wise vectors. Each sensor provides three orthogonal measurements, forming an expanded feature space:

$$S_{\text{expanded}} = \{a_x, a_y, a_z,\ l_x, l_y, l_z,\ g_x, g_y, g_z,\ m_x, m_y, m_z\}$$

Here, a_x, a_y, a_z denote the three-axis accelerometer data; l_x, l_y, l_z represent the linear acceleration in three axes; g_x, g_y, g_z correspond to the gyroscope data; and m_x, m_y, m_z are the three-axis magnetometer readings. This separation operation expands the original three-dimensional sensor data into a 12-dimensional feature space, significantly enriching the informational dimensions available for analysis.

By applying this separation approach, the algorithm can access and utilize specific signal patterns captured by different sensors along different axes. For example, the Z-axis acceleration is highly sensitive to vertical impact during foot strikes, while the Y-axis of the gyroscope may better capture body rotation during walking. These separated signal sources serve as a rich basis for subsequent optimized combinations.

The data flow of the traditional method is illustrated as:

Sensor Data (3-axis) → Composite Magnitude → Signal Processing → Peak Detection

In contrast, the data flow in this method is:

Sensor Data (Multi-sensor, Multi-axis) → Axis Separation → Optimal Combination Selection → Signal Processing → Peak Detection

The fundamental difference in these workflows lies in the timing of dimensionality compression. Traditional methods perform early-stage fusion, compressing the three-axis data into a single magnitude value. In contrast, the proposed method preserves the original dimensionality of the signal as much as possible, deferring dimensionality reduction until the optimal combination stage, thereby allowing for more flexible and informative signal integration.

3.3.2.3 The theoretical basis of axis combination

The selection of multi-sensor axis combinations is guided by the following theoretical considerations:

Different sensors exhibit complementary strengths in capturing motion characteristics. Accelerometers are effective in measuring linear acceleration and are sensitive to impacts and gravity; linear accelerometers isolate pure linear acceleration by removing gravitational components; gyroscopes specialize in angular velocity, capturing rotational motion; and magnetometers offer directional reference relative to the Earth's magnetic field. By integrating data from various sensor types, a more comprehensive and multidimensional representation of motion features can be achieved.

Both theoretical analysis and experimental validation suggest that, for the task of step detection, utilizing three independent signal sources is generally sufficient to provide the necessary information dimensionality. This "three-dimensional combination" strategy strikes an effective balance between feature completeness and computational efficiency.

Signal-to-noise ratios vary across axes depending on walking condition and sensor placement. For instance, when the device is worn at the waist, the vertical (Z-axis) acceleration signal tends to have a higher signal-to-noise ratio; whereas when carried in a trouser pocket, linear acceleration along the anterior-posterior direction (Y-axis) may offer clearer step-related features. Selecting the axes with the highest signal-to-noise ratios can enhance the stability and precision of detection.

To align with computational efficiency and real-world applicability, a pre-screening strategy based on prior knowledge is employed. According to experimental findings , several representative and high-potential combinations are pre-selected. These include homogeneous three-axis groupings from a single sensor type (e.g., X, Y, and Z axes of the accelerometer), as well as heterogeneous combinations across sensor types (e.g., X-axis of the accelerometer, Y-axis of the linear accelerometer, and Z-axis of the gyroscope).

3.3.2.4 Signal processing framework

For the selected axis combination, the algorithm follows a systematic signal processing framework, which includes the following core step:

1. Composite Magnitude Calculation: Compute the fused magnitude from the three chosen signal sources:

$$M_{\text{fusion}}(t) = \sqrt{S_1^2(t) + S_2^2(t) + S_3^2(t)} \tag{3.16}$$

   Here, S_1, S_2, and S_3 represent the three selected directional signals. A key distinction from traditional approaches lies in the fact that these signals are not restricted to the three axes of a single sensor. Instead, they can originate from different axes across multiple sensors, enabling cross-sensor information fusion.

2. Multi-stage Signal Filtering: Sensor signals collected during walking often contain various types of noise and interference across different frequencies. To isolate the meaningful components, this method adopts a structured three-stage filtering process.

   First, a median filter is applied to eliminate spikes and outliers, which are typically caused by sudden sensor jitter or external disturbances. Second, a low-pass filter is used to suppress high-frequency noise while retaining the low-frequency components associated with human gait. Finally, a moving average filter is employed to further smooth the signal waveform, enhancing the periodic features of walking steps.

   This multi-stage filtering strategy effectively reduces diverse noise artifacts and improves the clarity and detectability of gait-related features.

3. Signal Normalization:The signal is centered by subtracting the mean value to eliminate the influence of static components such as gravitational bias and highlight dynamic variations:

$$M_{\text{norm}}(t) = M_{\text{smooth}}(t) - \mu_M$$

   where μ_M represents the mean value of the smoothed signal. This step is particularly important because it removes the gravitational offset caused by the sensor's placement, making the algorithm less sensitive to the device orientation.

4. Adaptive Thresholding: An adaptive threshold λ is determined based on the statistical properties of the signal to accommodate different walking styles and signal intensities:

$$\lambda = \alpha \cdot \sigma_M$$

   where σ_M is the standard deviation of the signal, reflecting the amplitude of fluctuations, and α is a scaling factor that adjusts the detection sensitivity. This adaptive method allows the algorithm to respond dynamically to variations caused by different walking behaviors or device positions.

5. Peak Detection and Validation: Peaks that exceed the threshold are further evaluated using temporal constraints based on human biomechanics:

$$T_{\text{min}} \leq \Delta t_{\text{step}} \leq T_{\text{max}}$$

   Here, Δt_{step} denotes the time interval between adjacent peaks. T_{min} and T_{max} define the allowable range, typically set to 0.35 s and 1.8 s, respectively, which correspond to a human walking cadence of approximately 0.5–2.5 Hz. This validation step helps exclude false positives and improve detection accuracy.

3.3.3 Method characteristics

Based on multi-sensor axis fusion, the proposed step detection method exhibits the following three key technical features and advantages:

1. Multi-dimensional Information Fusion and Complementarity: By separating and recombining the axis data from multiple sensors, this method achieves effective integration of multi-dimensional information. Different sensors capture distinct motion characteristics that are mutually comple-

mentary: accelerometers reflect linear movement but are affected by gravity; linear accelerations exclude gravitational components; gyroscopes capture rotational dynamics; magnetometers offer directional cues. The intelligent combination of these complementary signals enables the algorithm to extract step features more comprehensively while avoiding the limitations of relying on a single sensor, thereby enhancing the discriminability and robustness of the signal features.

2. Adaptive and Intelligent Design: The algorithm automatically adjusts detection parameters through adaptive thresholding based on signal statistics, accommodating variations in walking styles, device placements, and environmental conditions without requiring manual calibration. In addition, the incorporation of human biomechanics verification enhances the accuracy of true step detection and reduces false positives caused by signal noise. This adaptive mechanism significantly improves algorithmic resilience in complex real-world scenarios.
3. Practicality and Efficiency Optimization: Although theoretically there may be numerous possible axis combinations, the method selects the most promising ones based on experimental validation and prior knowledge to ensure high detection accuracy while controlling computational complexity. Furthermore, the algorithm demonstrates strong adaptability across various device placements (e.g., handheld, pocket, or waist-mounted), making it suitable for diverse mobile usage contexts. This balance of efficiency and robustness ensures reliable operation on resource-constrained mobile devices in dynamic real-world applications.

3.4 The research method of Step length used

Step length estimation plays a critical role in PDR systems, directly impacting positional calculation accuracy. This research implements an enhanced Weinberg non-linear model for step length estimation, which incorporates human biomechanical properties while preserving computational efficiency.

The traditional Weinberg[37] model bases step length estimation on vertical acceleration changes during ambulation, with its fundamental hypothesis being that vertical displacement of the human body's center of mass is proportionally related to step length. This displacement can be indirectly quantified through the oscillation magnitude of acceleration signals. The mathematical formulation of the conventional Weinberg model is expressed as:

$$SL = K \times \sqrt[4]{(a_{max} - a_{min})} \tag{3.17}$$

Where SL denotes the estimated step length, K represents a calibration constant typically associated with pedestrian height, and a_{max} and a_{min} respectively correspond to the maximum and minimum acceleration signal values within a single gait cycle.

This research utilizes an optimized Weinberg model[38] that enhances estimation accuracy by simultaneously integrating height characteristics, cadence variations, and acceleration properties. The improved framework initially establishes a foundation step length based on pedestrian height:

$$Base\_SL = \alpha \times H \tag{3.18}$$

where H represents the pedestrian's height and α denotes the height proportion coefficient.

Subsequently, the model incorporates a comprehensive multi-factor adjustment mechanism:

$$SL = Base\_SL \times F_{accel} \times F_{freq} \tag{3.19}$$

F_{accel} represents the acceleration adjustment factor, derived through normalization of acceleration differentials:

$$F_{accel} = 0.85 + 0.3 \times \frac{Accel\_diff - Accel\_diff_{min}}{Accel\_diff_{max} - Accel\_diff_{min}} \tag{3.20}$$

F_{freq} denotes the cadence adjustment factor, determined by comparing current step frequency against mean step frequency. Finally, to ensure the rationality of estimated stride length, boundary constraints are implemented:

$$min\_SL \leq SL \leq max\_SL \tag{3.21}$$

The optimized Weinberg stride length estimation methodology offers multiple advantages: it accommodates various locomotion states and device carrying configurations through its multi-factor adjustment framework; the height-based fundamental stride length configuration ensures estimates align with individual characteristics; its computational efficiency makes it well-suited for real-time processing on mobile platforms; it eliminates dependency on pre-calibration procedures requiring known total distances, enabling immediate implementation across diverse environments; furthermore, through normalization processing and rationality constraints, it effectively mitigates the influence of outliers and noise interference.

3.5 The research method of heading estimation used

3.5.1 The basic principle of heading estimation without attitude constraints

Traditional PDR heading estimation approaches typically require smartphones to maintain fixed relative positioning with respect to pedestrians, significantly constraining system applicability in practical scenarios. In everyday contexts, users may place their devices in pockets, hold them while reading, position them against ears during calls, and so forth, resulting in frequent misalignments between device heading and actual pedestrian movement direction. This research employs the posture-unconstrained heading estimation methodology proposed by Donghui Liu et al.[14], which addresses this challenge by enabling PDR systems to accommodate multiple device holding configurations. The fundamental concept underlying this approach involves coordinate system rotational transformation, whereby the smartphone's body coordinate system (carrier coordinate system) undergoes realignment to orient one of its axes with the pedestrian's actual progression direction. This coordinate transformation alignment approach enables heading estimation to function independently of users maintaining particular smartphone orientations, substantially enhancing system convenience and applicability in practical scenarios.

The key to implementing this methodology lies in utilizing frequency domain characteristics of acceleration signals during pedestrian locomotion. Research has established that during human walking, acceleration signals along the progression direction exhibit prominent peaks at step frequency, resulting from forward acceleration and deceleration generated with each step; conversely, acceleration signals perpendicular to the walking direction display significant peaks at half-step frequency, corresponding to the lateral oscillation pattern where the human body completes one side-to-side movement every two steps[39][40]. The axis perpendicular to the ground likewise exhibits peaks at step frequency, though typically with amplitude substantially greater than peaks along the walking direction axis.

Based on these distinctive frequency domain characteristics, this research employs rotational traversal to identify a novel coordinate system configuration that effectively aligns a specific smartphone axis with the pedestrian's actual walking direction. This alignment is accomplished through mathematical transformation rather than requiring users to physically hold the device in predetermined orientations.

3.5.2 Implementation of Heading Estimation Algorithm

The implementation of this attitude constraint-free heading estimation algorithm includes the following key steps:

3.5.2.1 Data acquisition and gait detection

Initially, raw data is collected from integrated smartphone sensors (accelerometer, gyroscope, and magnetometer). Although heading estimation primarily utilizes acceleration data, attitude computation requires information from all three sensor types. The system employs a gait detection module to identify the temporal markers of individual steps, providing reference points for subsequent analysis. The sampling rate is configured at 100Hz to ensure accurate capture of human locomotion characteristics.

3.5.2.2 Three-axis rotation traversal determines the optimal coordinate system

Following data collection and preprocessing, to identify optimal alignment between the smartphone coordinate system and walking direction, the algorithm executes a three-step rotational angle traversal:

1. X-axis rotation traversal:
    - Rotate acceleration data around the X-axis from $0°$ to $90°$
    - At each angle, apply low-pass filtration to eliminate high-frequency interference
    - Transform data to frequency domain via FFT, identifying the axis with maximum peak at step frequency
    - Record optimal rotation angle θ_x
2. Y-axis rotation traversal:
    - Initially rotate by angle θ_x around X-axis
    - Subsequently rotate around Y-axis from $0°$ to $90°$
    - Repeat the aforementioned frequency domain analysis procedure
    - Record optimal rotation angle θ_y
3. Z-axis rotation traversal:
    - First rotate around X-axis and Y-axis by angles θ_x and θ_y respectively

- Then rotate around Z-axis from $0°$ to $90°$
- Calculate peak value ratios at step frequency and half-step frequency for each axis
- Identify walking direction axis based on these ratios
- Record optimal rotation angle θ_z

To enhance computational efficiency, Donghui Liu employed binary search methodology to rapidly approximate optimal angles rather than examining all possible values. However, this approach potentially converges incorrectly to local optima; consequently, this research implements grid search methodology.

3.5.2.3 Coordinate system transformation and filtering processing

After identifying the optimal rotation angles (θ_x, θ_y, θ_z), construct a rotation matrix to transform the original accelerometer data:

$$C_{\alpha}^{\beta} = \begin{pmatrix} \cos\psi & -\sin\psi & 0 \\ \sin\psi & \cos\psi & 0 \\ 0 & 0 & 1 \end{pmatrix} \begin{pmatrix} \cos\gamma & 0 & \sin\gamma \\ 0 & 1 & 0 \\ -\sin\gamma & 0 & \cos\gamma \end{pmatrix} \begin{pmatrix} 1 & 0 & 0 \\ 0 & \cos\theta & -\sin\theta \\ 0 & \sin\theta & \cos\theta \end{pmatrix} \tag{3.22}$$

Where ψ, γ and θ correspond to rotation angles around the Z, Y and X axes respectively.

Following rotation, apply differentiated filtering procedures to distinct axes:

- For walking direction axis: Implement low-pass filtration with cut-off frequency marginally exceeding step frequency
- For axis perpendicular to walking direction: Apply band-pass filtration to extract components proximate to step frequency
- For axis perpendicular to ground: Utilize matched filtering to extract meaningful signal components

This differentiated filtration strategy enhances preservation of relevant information across each axis while simultaneously eliminating noise interference.

3.5.2.4 Attitude calculation and geographic coordinate system projection

After obtaining coordinate system data aligned with pedestrian walking direction, projection of this data into the geographic coordinate system becomes necessary. The Attitude Heading Reference System (AHRS) processes rotated sensor data to calculate the orientation of the transformed coordinate system relative to the geographic reference frame. This AHRS framework integrates information from gyroscope, accelerometer, and magnetometer sensors, representing orientation through quaternions or direction cosine matrices. The current research implements a QEKF-AHRS methodology—specifically, an Attitude Heading Reference System based on quaternion extended Kalman filtering—to determine orientation parameters.

Utilizing attitude information computed by AHRS, construct a transformation matrix C_n^b [41]from the rotated coordinate system to the geographic coordinate system, then project the post-rotation acceleration data into the geographic coordinate framework:

$$a^n = C_n^b \cdot a_{filtered}^b \tag{3.23}$$

Where a^n represents acceleration within the geographic coordinate system, and $a^b_{filtered}$ denotes filtered acceleration in the rotated body coordinate system.

3.5.2.5 Heading Angle calculation

This methodology does not employ a strategy of calculating heading for each individual step, but instead performs computation every two steps to eliminate the influence of lateral oscillation movements during walking. Integration is applied to geographic coordinate system acceleration data between every two steps:

$$v(t) = \int_{t_1}^{t_2} a^n(t)dt \tag{3.24}$$

Where t_1 and t_2 represent the temporal points of consecutive steps.

Finally, calculate the heading angle from the velocity vector:

$$\phi = \arctan 2(v_E, v_N) \tag{3.25}$$

Where v_E and v_N denote eastward and northward velocity components respectively, and ϕ represents the heading angle relative to true north direction.

Through this implementation process, the posture-unconstrained heading estimation algorithm accommodates diverse smartphone holding configurations, endowing PDR systems with enhanced flexibility and practicality for real-world implementations, enabling effective functionality across varied usage scenarios.

3.6 The principle of complementary filtering

In this study, we implemented a Complementary Filter as our methodology for multi-source data fusion to effectively integrate PDR and WiFi positioning information. The Complementary Filter represents a streamlined and efficient approach to information fusion, particularly well-suited for combining sensor data with complementary characteristics.

The fundamental principle of the Complementary Filter leverages the frequency-domain complementary properties of different sensors. Specifically, one sensor type may perform exceptionally well within certain frequency ranges while showing diminished performance in others. Conversely, another sensor type exhibits opposite performance characteristics across different frequency ranges. Through this complementarity, the filter extracts the most reliable information components from each data source, achieving optimized fusion.

In the context of PDR and WiFi positioning integration, the PDR system delivers continuous relative position change information with high short-term accuracy but suffers from long-term cumulative errors. Meanwhile, WiFi positioning provides absolute position references that, despite potentially lower instantaneous precision, do not accumulate errors over time. The characteristics of these two technologies perfectly complement each other: PDR demonstrates excellent performance over brief intervals, while WiFi positioning maintains stability over extended time scales.

The mathematical expression of the Complementary Filter is as follows:

$$P_f(t) = \alpha \cdot [P_f(t-1) + P_{PDR}(t) - P_{PDR}(t-1)] + (1-\alpha) \cdot P_{WiFi}(t) \tag{3.26}$$

Where:

- $P_f(t)$ represents the fused position estimate at the current time t
- $P_f(t-1)$ represents the fused position estimate at the previous time $t-1$
- $P_{PDR}(t)$ and $P_{PDR}(t-1)$ respectively represent the PDR position estimates at the current time and previous time
- $P_{WiFi}(t)$ represents the WiFi position estimate at the current time
- α is the fusion weighting coefficient ($0 < \alpha < 1$), used to balance the contribution of PDR and WiFi information

In this formula, the first component $P_f(t-1)+P_{PDR}(t)-P_{PDR}(t-1)$ represents the position increment update obtained through PDR, reflecting short-term position changes; the second component $P_{WiFi}(t)$ provides absolute position reference for correcting cumulative errors. The selection of parameter α is critically important: when PDR performs effectively (such as during straight-line walking), a larger α value can be assigned; after complex movements or extended walking periods, the α value should be reduced to increase the influence of WiFi positioning.

Compared to complex algorithms such as Kalman filtering, the Complementary Filter offers advantages including lower computational burden and simpler implementation, making it particularly suitable for real-time operation on resource-constrained mobile devices. Through this method, we can effectively combine the high-precision short-term tracking capability of PDR with the long-term stability of WiFi positioning, ultimately enhancing overall positioning performance.

3.7 summary of Methodological Framework

This research explores a pedestrian dead reckoning methodology that attempts to mitigate common orientation constraint issues in smartphone-based positioning. The approach integrates three complementary principal components to form a comprehensive framework:

The gait detection algorithm employs a multi-sensor axis fusion approach, utilizing data from various sensors embedded within smartphones. By decomposing sensor signals into three-axis components and examining different combinations of these components, the system endeavors to enhance step recognition across varying device orientations. This methodology treats each axis of every sensor as an independent information source, potentially achieving more robust gait identification than conventional approaches that rely on composite signals from individual sensors.

Regarding stride length estimation, the study implements an enhanced Weinberg model, seeking to balance computational efficiency with estimation accuracy. This approach establishes a personalized baseline stride length correlated with user height, adjustable through acceleration differential and cadence factors. The introduction of adaptive thresholds and boundary constraints may contribute to maintaining reasonable estimates across different walking patterns.

Heading estimation utilizes frequency domain analysis to facilitate walking direction identification, reducing device orientation constraints. Through coordinate transformation and axis rotation traversal, the system attempts to align smartphone axes with actual walking direction based on characteristic frequency patterns rather than physical orientation. Nevertheless, challenges posed by magnetic interference[42][43] in indoor environments warrant attention.

3.8 Experimental Design

3.8.1 Experimental environment and path planning

This investigation utilized corridors within the Cyprus University of Technology (CUT) academic facility as the experimental location, as depicted in Figure 3.7. This setting exemplifies a representative indoor environment with defined corridor configurations, homogeneous lighting parameters, and consistent floor surfaces, rendering it suitable for evaluating pedestrian navigation system efficacy. Furthermore, the academic facility houses numerous electronic devices and reinforced concrete structural elements that introduce magnetic field interferences, establishing ideal circumstances for examining the resilience of the posture-unconstrained heading estimation algorithm.

Figure 3.7: geographic coordinate system

The experimental trajectory design was conceived to encompass archetypal pedestrian locomotion scenarios, incorporating both rectilinear movement and turning as fundamental motion patterns. The pathway configuration adopts an inverted “Z” morphology, specifically comprising three discrete segments:

1. Initial segment: Commencing from the origin coordinates (0,0) and proceeding in a direction 50° northeast for a distance of 32 meters
2. Intermediate segment: Reorienting toward 40° northwest (corresponding to 320° northeast) and traversing 11 meters
3. Terminal segment: Executing a subsequent directional adjustment to 50° northeast and continuing

for an additional 11 meters

This tripartite trajectory architecture necessitates that participants execute two pronounced directional transitions, rigorously challenging the heading estimation algorithm's capabilities under conditions of dynamic variation. Furthermore, the incorporation of pathway sections with heterogeneous lengths facilitates comprehensive evaluation of step length estimation algorithm reliability and accuracy across varied ambulatory distances.

3.8.2 Experimental Equipment and Data Acquisition

This investigation employed a OnePlus 10 Pro smartphone as the experimental apparatus, featuring integrated MEMS sensors comprising triaxial accelerometer, triaxial gyroscope, and triaxial magnetometer components. The AndroSensor application facilitated sensor data acquisition throughout experimental procedures. This software simultaneously records multiple sensor parameters and synchronously preserves information in analytically compatible formats. To guarantee acquisition fidelity, sampling frequencies for all sensors were configured at 100Hz, enabling detection of subtle variations during human ambulation processes. The acquired dataset encompasses:

- Acceleration measurements (a_x, a_y, a_z)
- Gyroscopic readings $(\omega_x, \omega_y, \omega_z)$
- Magnetometer values (m_x, m_y, m_z)
- Linear acceleration parameters (gravity component excluded)
- Temporal timestamp information

3.8.3 Experimental Procedure and Test Plan

This research designed two distinct smartphone carrying configurations to evaluate the adaptability of the posture-unconstrained heading estimation algorithm:

1. Pocket Mode: The OnePlus 10 Pro was positioned within trouser pockets, simulating the most prevalent smartphone carrying method during routine pedestrian movement. Under this configuration, the device orientation remains relatively consistent relative to the body but experiences subtle movements during walking, while the smartphone coordinate system maintains no fixed relationship with the walking direction.
2. Reading Mode: Test participants held the smartphone with both hands while maintaining the screen oriented toward themselves, replicating scenarios where users view device content while walking. In this configuration, the smartphone exists in a comparatively dynamic state, experiencing additional oscillations and orientation changes resulting from hand movements.

To ensure experimental data consistency and reliability, all trials were conducted by a single test participant, following this procedural protocol:

1. Initializing the data acquisition system at the starting position
2. Traversing the designated path with natural gait while maintaining relatively consistent walking speed
3. Terminating data collection upon reaching the endpoint

4. Repeating the aforementioned test procedure minimum three times for each carrying configuration to mitigate the influence of random errors

To evaluate the performance of integrated PDR-WiFi fusion positioning, additional WiFi fingerprinting activities were conducted:

1. Establishing WiFi sampling locations at 2-meter intervals along the experimental trajectory
2. Remaining stationary for approximately 20 seconds at each sampling location to acquire Received Signal Strength Indicator (RSSI) measurements from surrounding WiFi access points
3. Performing multiple acquisition sessions at identical locations across different temporal periods to account for signal strength temporal variability characteristics
4. Constructing mapping relationships between spatial coordinates and WiFi fingerprints to facilitate subsequent development and validation of PDR-WiFi fusion positioning algorithms

3.8.4 Evaluation Indicators and Verification Methods

To comprehensively evaluate the proposed methodology's performance, this research employs the following metrics for quantitative analysis:

1. Gait detection accuracy: Comparing algorithm-detected step count against actual step count to calculate detection precision
2. Heading estimation error: Computing average directional deviation between estimated and ground truth heading values
3. Trajectory reconstruction error: Measuring positional discrepancies between PDR trajectories and actual paths, encompassing mean positioning error and endpoint deviation
4. Posture adaptability indicator: Examining metric variations across different carrying configurations to assess algorithmic adaptability to diverse orientations
5. Pre-fusion versus post-fusion trajectory error: Conducting comparative analysis of positional deviations between PDR trajectories and actual paths before and after WiFi integration, focusing on mean positioning error

Through these indicators, comprehensive performance assessment of the proposed methodology across multiple dimensions becomes achievable.

4 Experimental Results and Discussion

4.1 result of Step detection

Figure 4.1 presents a comparative visualization between unprocessed sensor signals and their filtered counterparts. During data acquisition, the original signals recorded in pocket mode (represented by blue lines) exhibited pronounced amplitude variations (ranging from 4 to 20), accompanied by significant noise characteristics and unstable signal quality. Following application of the multi-stage filtration techniques outlined in Chapter 3, the enhanced signals (depicted by red lines) demonstrated notable smoothing properties, with amplitude effectively constrained within the 8 to 14 range, while successfully preserving gait periodicity features, thereby establishing a dependable foundation for subsequent peak detection algorithms. Temporal domain examination revealed that throughout the entire 55.4 seconds experimental duration, the signal maintained consistently stable periodic fluctuations, closely corresponding with typical human walking patterns. The processed signal, through mean value reconstruction, comprehensively retained the fundamental trends of the original data while effectively suppressing random perturbation factors, thus substantially improving the signal-to-noise ratio performance.

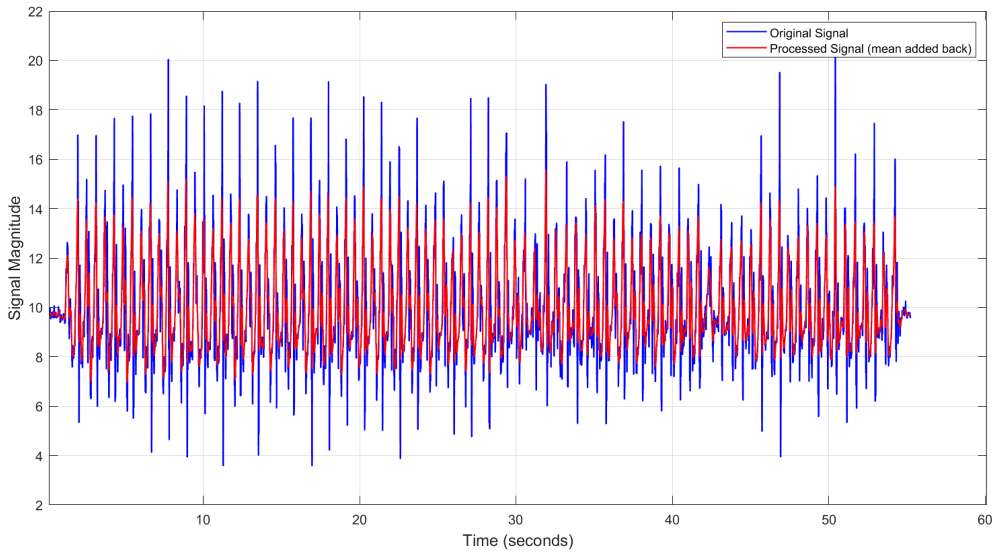

Figure 4.1: The processed signal (pocket mode)

Figure 4.2 illustrates the steps detection results in pocket mode. The optimal sensor axis configuration, Accel_X-Accel_Y-Lin_Acc_Z, successfully identified 89 steps, which corresponds precisely with the actual step count. As observable in the figure, the detected peak points (marked by red circles) are distributed with remarkable consistency throughout the temporal sequence, demonstrating the algorithm's robust capability to recognize stride characteristics across various time intervals. The adaptive threshold (indicated by a red dashed line) positioned at approximately 0.6 effectively differentiates authentic stride peaks from background oscillations. During the step identification procedure, the algorithm executed peak recognition after eliminating the signal's mean value, thereby directing the detection process toward the dynamic fluctuations within the signal rather than absolute magnitudes.

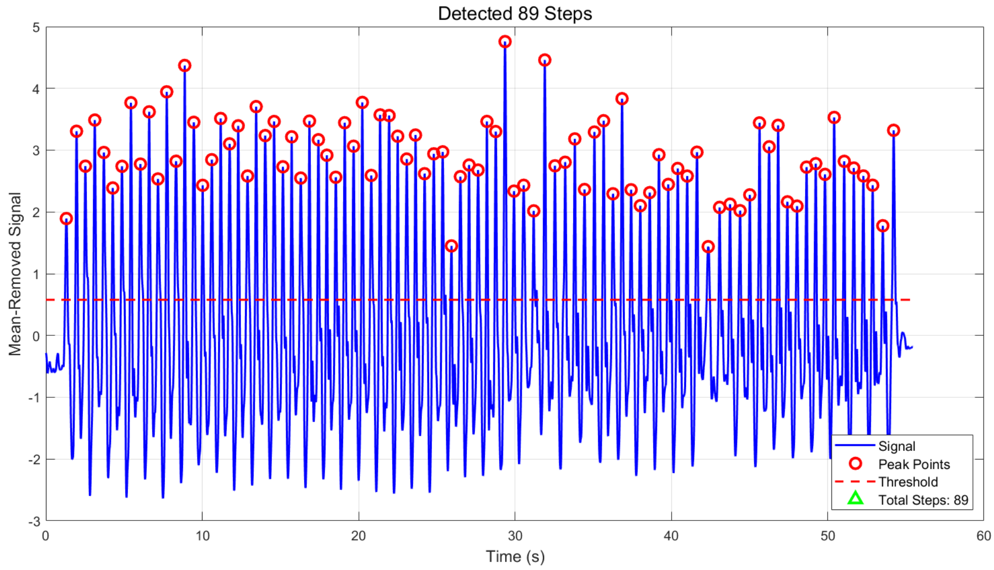

Figure 4.2: steps detection results (pocket mode)

Figure 4.3 displays the signal processing outcomes in reading mode. Compared to pocket mode, the original signals in reading mode exhibit a more pronounced amplitude growth trajectory, particularly during the latter testing phase (40-78.9 seconds), where signal magnitude increases from an initial value of approximately 7 to roughly 10 in the final stages. This progression indicates that the user's walking pattern gradually transitions into a more stabilized state during reading mode, with arm oscillations becoming increasingly uniform. The processed signal (represented by the red line) effectively preserves this developmental pattern while simultaneously providing enhanced gait cycle characteristics through filtration techniques.

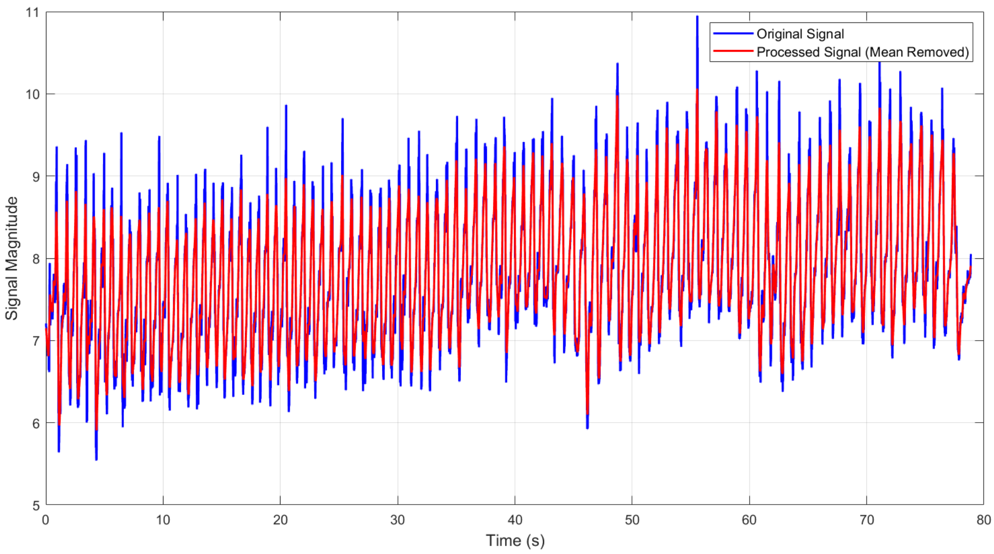

Figure 4.3: The processed signal (reading mode)

Figure 4.4 illustrates the step detection results in reading mode utilizing the Accel_X-Accel_Y-Lin_Acc_Z sensor axis configuration. Under this arrangement, the algorithm identified 92 steps, which aligns with the actual step count. Notably, the step signal demonstrates progressively increasing amplitude during the latter testing phase (30-78.9 seconds), with peak intensity growing from approximately 0.8 in the initial stages to roughly 2.0 toward the conclusion. The peak detection algorithm, employing an adaptive threshold (approximately 0.3), successfully accommodated these amplitude variations, demonstrating the methodology's excellent adaptability in processing non-stationary walking signals. The detection outcomes reveal that despite significant amplitude fluctuations, the identified steps maintain uniform and continuous distribution without evident missed detections or false positives, thereby confirming the algorithm's robustness in dynamic environments.

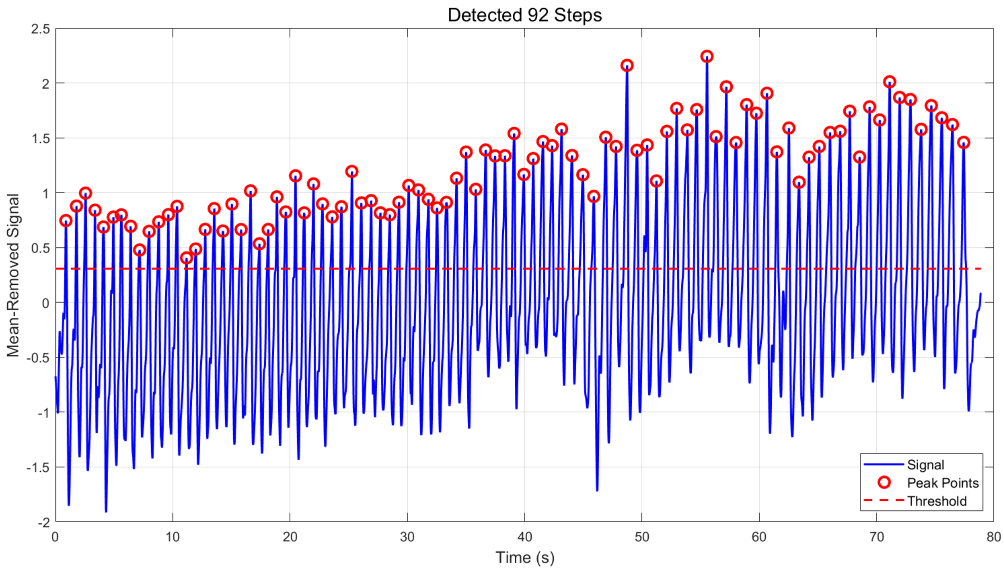

Figure 4.4: steps detection results (reading mode)

The experimental findings reveal significant performance variations among different sensor axis configurations. Conventional methodologies typically employ only the composite three-axis signal from a single sensor (such as an accelerometer) for step detection, whereas the multi-sensor axis combination approach developed in this research demonstrates substantial advantages. Notably, the Accel_X-Accel_Y-Lin_Acc_Z configuration exhibited superior performance in this investigation, ingeniously leveraging the complementary characteristics of diverse sensors. In contrast, configurations utilizing exclusively single-type sensors, such as solely accelerometer triaxial or magnetometer triaxial arrangements, demonstrated diminished effectiveness. Testing results indicate that single-sensor methodologies typically produce step count discrepancies within the 10-20% range, whereas the cross-sensor axis combination strategy successfully constrains error margins to within 3%, thereby validating the efficacy of the integrated sensor axis approach.

4.2 result of Step length estimation

Figure 4.5 illustrates stride length variations in pocket mode. The estimation employs an enhanced Weinberg non-linear model, which integrates human biomechanical properties by simultaneously considering height, acceleration differentials, and cadence. As depicted, the estimated stride lengths in pocket mode exhibit pronounced dynamic variability, ranging from 0.52 to 0.76 meters, with an average stride length of 0.65 meters. The stride length trajectory demonstrates notable fluctuation characteristics, particularly evidenced by several distinct peaks (approximately 0.75 meters) between steps 30-50, while the 50-70 step interval displays reduced stride measurements (approximately 0.53-0.57 meters). This variation pattern reflects natural gait adjustments during ambulation and corresponds closely with the oscillatory characteristics of acceleration signals throughout the walking process.

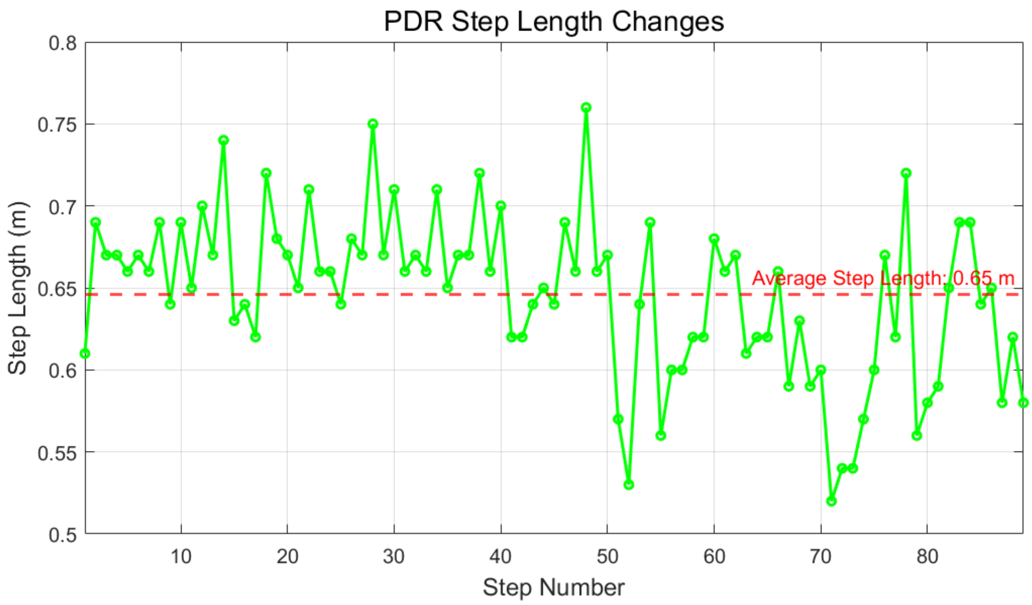

Figure 4.5: result of steps length estimation (pocket mode)

Figure 4.6 presents the stride length estimation results in reading mode. Compared to pocket mode, stride lengths in reading mode are generally shorter, with an average value of 0.57 meters and variations ranging from 0.48 to 0.67 meters. The stride length curve in reading mode exhibits a distinct downward trajectory during the initial phase (first 5 steps), rapidly declining from approximately 0.67 meters to around 0.55 meters, reflecting the user's transition from the starting phase to a stabilized walking state. During the middle and later phases (steps 30-92), stride length fluctuations remain relatively consistent, with most measurements maintained between 0.54 and 0.60 meters, exhibiting only brief significant reductions (approximately 0.49 meters) at specific intervals, such as near steps 50-55.

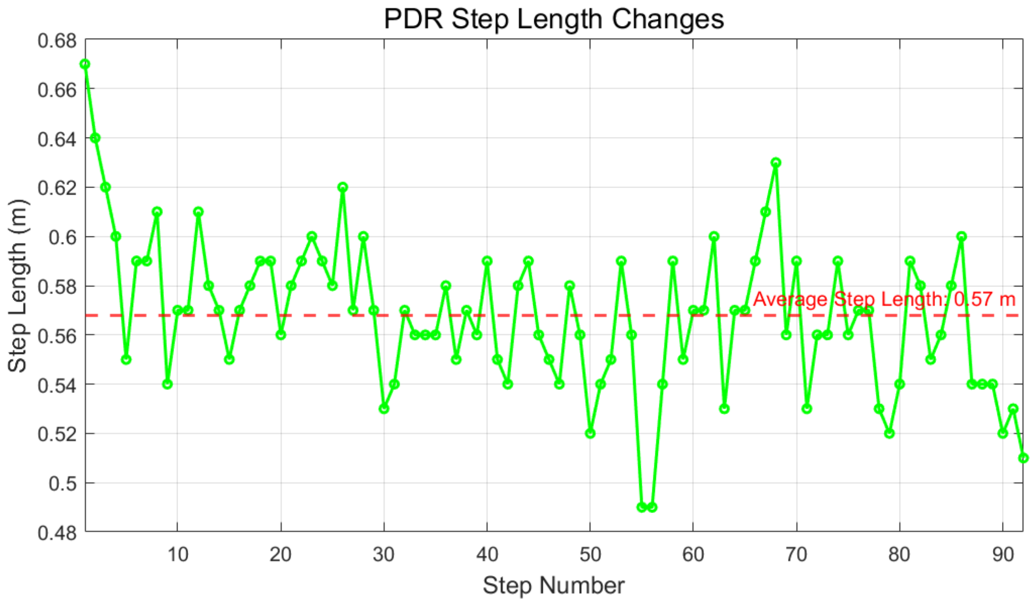

Figure 4.6: result of steps length estimation (reading mode)

Comparing the stride length estimation outcomes across both modes reveals several key distinctions: First, the average estimated stride length in pocket mode (0.65 meters) significantly exceeds that of reading mode (0.57 meters), representing an approximate difference of 14%; Second, the standard deviation of stride lengths in pocket mode (0.048 meters) surpasses that of reading mode (0.032 meters), indicating greater variability in the former; Third, stride length distribution in pocket mode appears more dispersed, whereas reading mode demonstrates a relatively concentrated distribution pattern. These observations suggest that device positioning methodology influences stride length estimation not only in terms of absolute values but also in the dynamic variation characteristics of stride measurements.

4.3 result of heading estimation

Figure 4.7 illustrates the heading angle estimation results generated by the posture-unconstrained heading estimation algorithm based on frequency domain analysis in pocket mode. This algorithm analyzes acceleration signal characteristics in the frequency domain, identifies walking direction, and achieves heading estimation independent of device orientation constraints by projecting acceleration onto the geographic coordinate system through coordinate transformation. As depicted, the estimated heading angles (blue line) maintain consistent overall trends with the ground truth heading angles (red line), effectively capturing directional transitions across three primary phases: the initial straight segment (steps 1-45, reference value 50°), the turning phase (steps 46-65, reference value 320°), and the final straight segment (steps 66-89, reference value 50°). During the initial phase, heading estimates exhibit considerable fluctuations ranging from approximately 30° to 100°; during the turning phase, the algorithm successfully recognizes directional changes albeit with some response latency; in the final phase, estimations display temporary overshoot phenomena before gradually converging toward reference values. The average heading estimation error in pocket mode measures 22.74°, which, although exceeding values reported in the original paper, still maintains practical utility considering the posture-unconstrained application scenario.

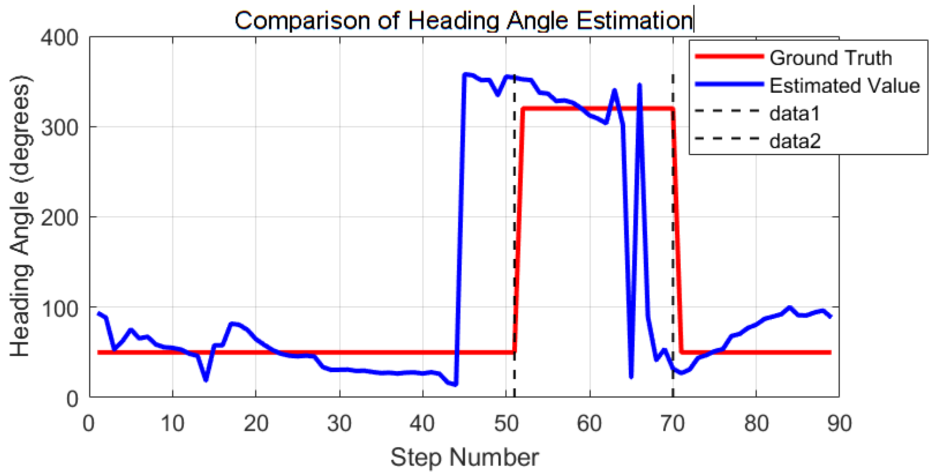

Figure 4.7: result of heading estimation (pocket mode)

Figure 4.8 presents the heading estimation results in reading mode. Compared to pocket mode, heading estimation in reading mode exhibits distinct characteristics: during the initial phase (steps 1-25), the estimates demonstrate relative stability; however, substantial fluctuations emerge within the step 25-55 interval, with estimates varying approximately 30° above and below the reference value; during the turning phase (steps 56-75), the algorithm displays exceptional response properties, rapidly tracking heading variations; in the final phase, estimated values also promptly recover to levels approaching the actual reference values. Overall, the average heading estimation error in reading mode measures 16.91°, representing a significant improvement compared to pocket mode, suggesting that acceleration signals in handheld conditions potentially provide more distinct directional features.

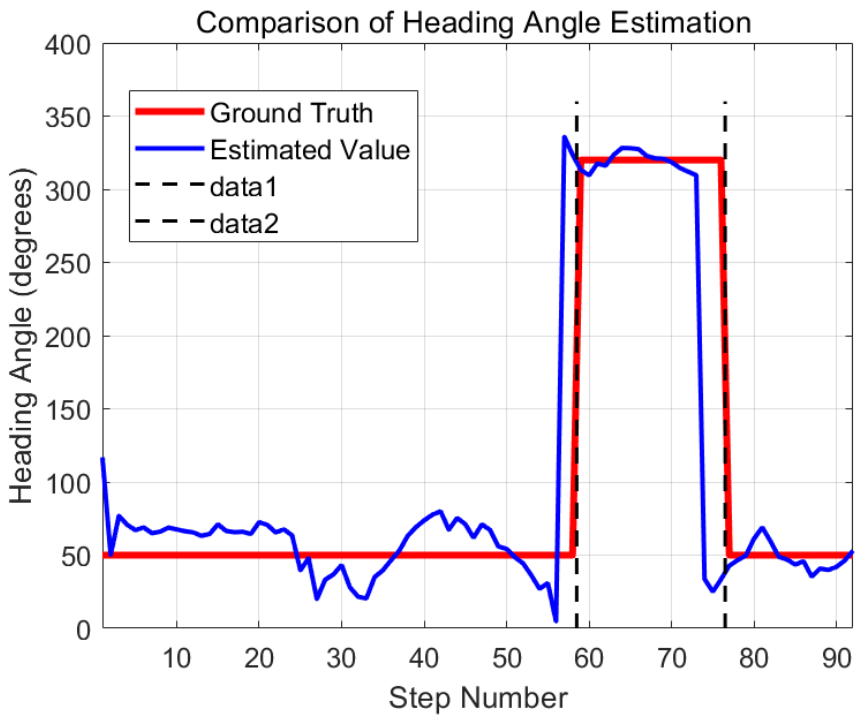

Figure 4.8: result of heading estimation (reading mode)

Experimental data indicates that heading estimation errors in this implementation are elevated compared to those reported in the original paper. This discrepancy may stem from multiple factors: initially, variations in experimental environments and equipment potentially affected acceleration signal quality; additionally, parameter adjustments in the code implementation may not have achieved optimal configuration; finally, differences in walking patterns and velocities could have influenced algorithm performance. Nevertheless, the current implementation still accurately captures overall heading variation trends in most scenarios, demonstrating a certain degree of methodological robustness.

Notably, heading estimations exhibit delayed responses at turning points, potentially attributable to the method's reliance on two-step integration for heading calculations. When pedestrians initiate turns, the integration window still contains partial data from linear walking segments, resulting in estimation lag. Furthermore, estimated values display significant deviations in certain step segments, suggesting that frequency domain feature identification may lack stability under specific conditions. These observations provide valuable direction for future algorithmic refinements.

Future enhancements could be pursued along several trajectories: (1) Refining frequency domain feature extraction methodologies, such as implementing wavelet transformation as an alternative to Fourier analysis, to more effectively capture non-stationary signal characteristics; (2) Developing adaptive parameter regulation mechanisms that dynamically optimize filter parameters according to detected locomotion states; (3) Incorporating machine learning technologies to recognize more sophisticated ambulation patterns and specialized movements (such as directional changes), thereby enhancing adaptability across diverse users and environmental contexts.

4.4 PDR and wifi integrated positioning

Figure 4.9 presents the PDR trajectory estimation results in pocket mode. As clearly observable in the illustration, the PDR trajectory maintains favorable consistency with the ground truth path during the initial walking phase; however, as step count increases, particularly after navigating the first turn (approximately at step 40), the trajectory begins to exhibit notable lateral deviation. This displacement partially recovers during the third path segment (NE 50°, 11m), ultimately resulting in approximately 1.58 meters of error between the final position (Step 89) and the actual endpoint. Significantly, while deviations exist in the pocket mode trajectory, it maintains relatively smooth characteristics overall, indicating that acceleration signals remain comparatively stable when the device is carried in a pocket, facilitating effective step frequency detection and heading estimation.

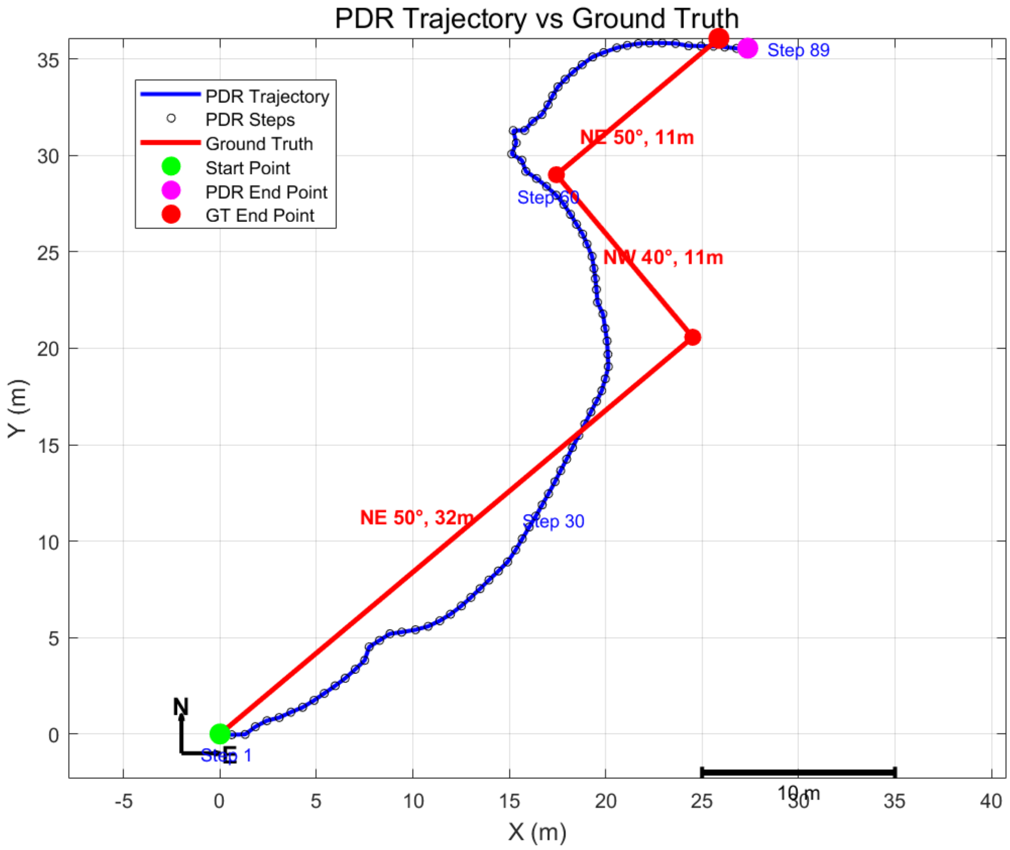

Figure 4.9: PDR trajectory (pocket mode)

Figure 4.10 illustrates the PDR trajectory estimation in reading mode. Compared to pocket mode, the reading mode trajectory demonstrates significant heading deviation during the first path segment (NE 50°, 32m), causing the entire route to systematically shift rightward. This initial discrepancy likely stems from subtle hand movements in reading mode interfering with accelerometer and magnetometer sensors, producing systematic errors in heading estimation. Directional patterns along the second (NW 40°, 11m) and third (NE 50°, 11m) path segments actually demonstrate considerable resemblance to the authentic route, indicating that estimations of relative heading changes achieve greater precision than absolute heading determinations. Nevertheless, due to accumulated deviations originating in the first segment, the final positional error reaches 5.27 meters, substantially exceeding that observed in pocket mode.

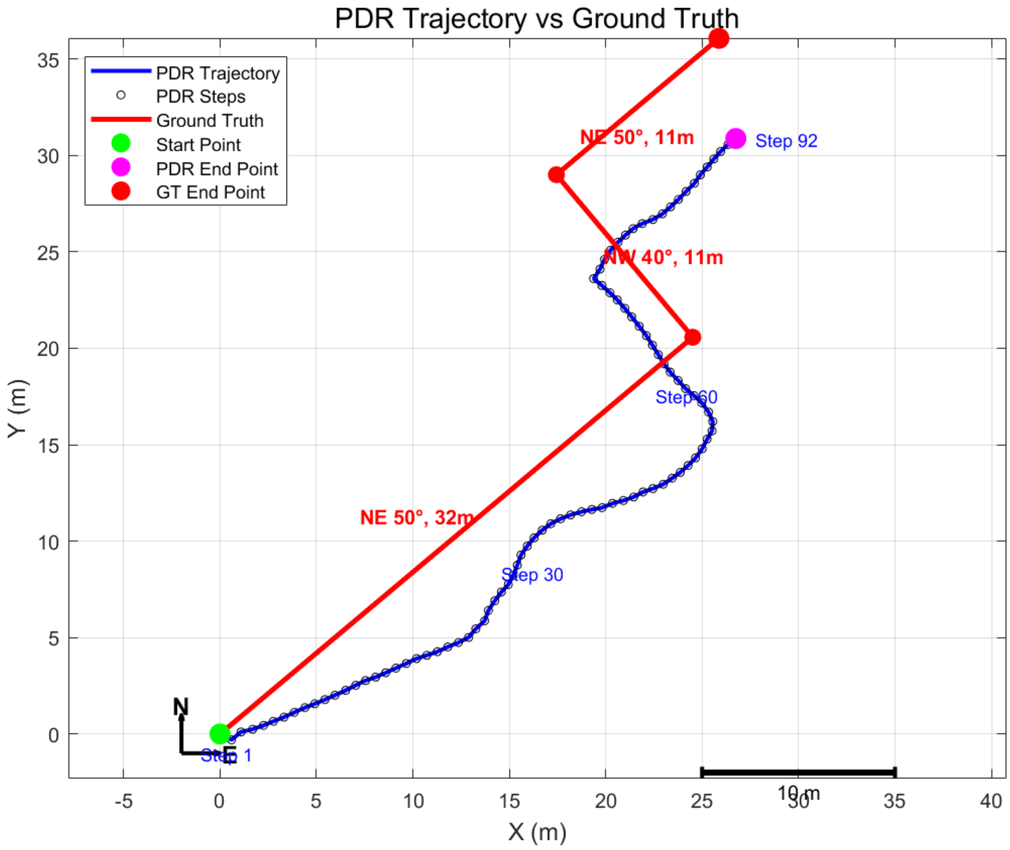

Figure 4.10: PDR trajectory (reading mode)

Figure 4.11 presents the localization performance of PDR integrated with WiFi positioning in pocket mode. The fused trajectory demonstrates remarkable enhancement, particularly in turning regions and segments following extended walking distances. The integration algorithm effectively mitigates PDR's cumulative errors through periodic WiFi reference coordinates, resulting in trajectories that more accurately correspond with ground truth values across the second and third path segments. Particularly noteworthy is the system's performance at the second turning point, where the fusion algorithm successfully captures directional transitions and accurately rectifies trajectory orientation, demonstrating the integrated system's exceptional adaptability to walking dynamic characteristics.

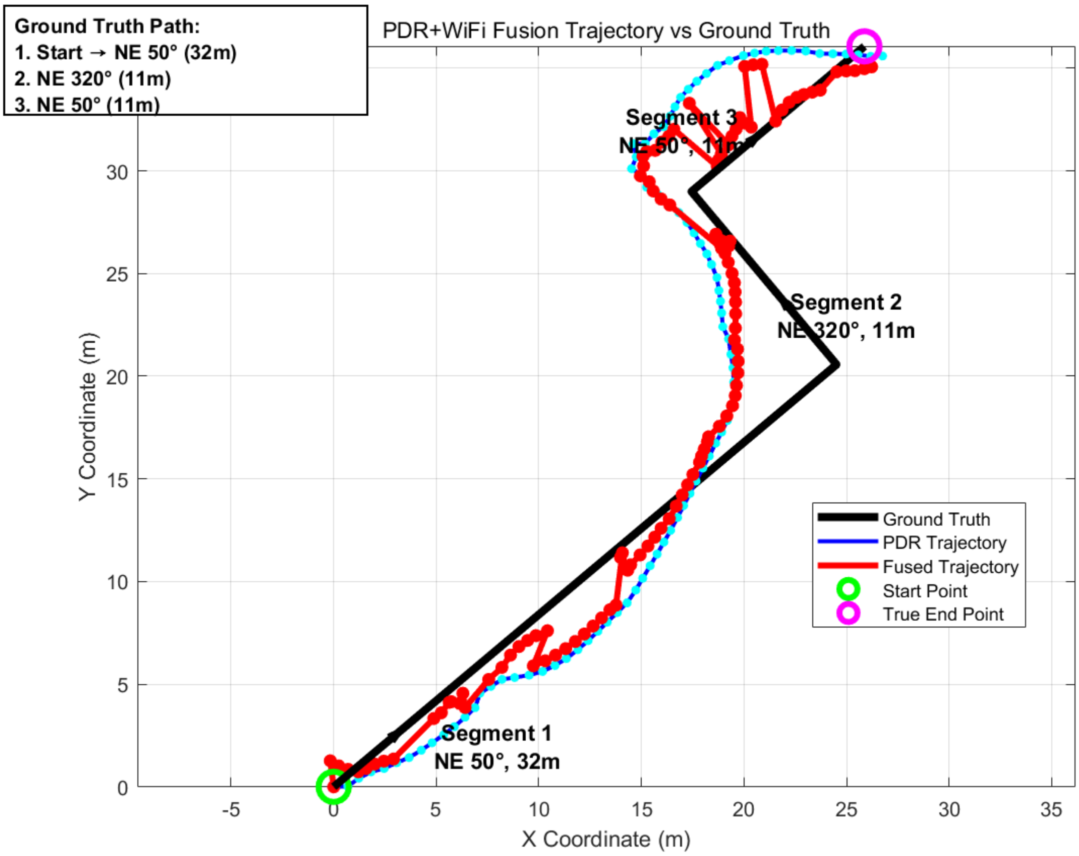

Figure 4.11: PDR and wifi integrated trajectory (pocket mode)

Figure 4.12 illustrates the fusion effects in reading mode, which appear particularly pronounced. The integration algorithm successfully diminishes systematic directional deviations in the initial segment, bringing the entire trajectory into closer alignment with the actual path. Notably, despite substantial divergence in the first segment of the original PDR trajectory, the fusion system progressively redirects the path toward proper orientation through WiFi reference coordinates. Throughout the second and third path segments, the integrated trajectory maintains excellent correspondence with ground truth values, achieving substantial corrective improvement.

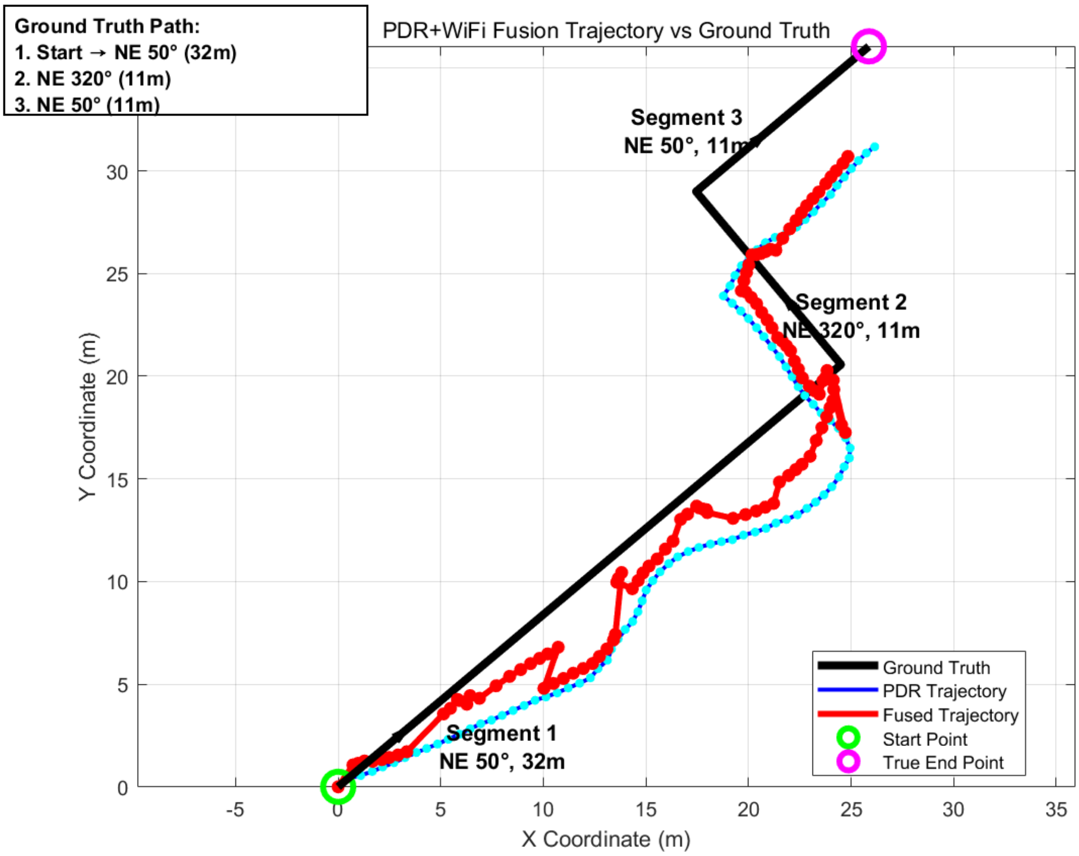

Figure 4.12: PDR and wifi integrated trajectory (reading mode)

Quantitative evaluation further validates the effectiveness of the fusion methodology. In pocket mode, the integration substantially diminishes average positioning error from 1.94 meters to 1.21 meters, representing an enhancement magnitude of 37.5%; in reading mode, mean error decreases from 2.51 meters to 1.59 meters, yielding a 36.6% improvement. This consistent enhancement magnitude demonstrates that the fusion algorithm exhibits robustness and adaptability across various device carrying configurations. The complementary filter-based integration strategy not only delivers substantial performance benefits but also offers advantages in computational efficiency and implementation simplicity, making it particularly appropriate for real-time applications on mobile devices with constrained resources.

Comprehensive analysis indicates that the complementary filter-based PDR-WiFi fusion methodology successfully integrates the strengths of both technologies, enhancing positioning accuracy across diverse usage scenarios while maintaining algorithmic elegance and computational efficiency.

5 Conclusion and Recommendations

5.1 Research Objectives and Abstract

This research addresses a significant technical challenge in smartphone-based Pedestrian Dead Reckoning (PDR) systems: conventional PDR algorithms typically require smartphones to maintain specific orientations for effective operation, substantially limiting their practical utility in everyday scenarios, as users naturally carry devices in various positions. The primary objective of this investigation is to develop and evaluate an adaptive pedestrian localization solution capable of functioning effectively across diverse smartphone carrying configurations without requiring users to maintain particular device orientations.

To accomplish this objective, the investigation explored three critical PDR components. Initially, a multi-sensor axis fusion methodology for step detection was implemented and evaluated, leveraging complementary information across various sensor types and axes. Subsequently, an enhanced Weinberg model was applied for stride length estimation, incorporating individual biomechanical characteristics while maintaining computational efficiency. Thirdly, a posture-unconstrained heading estimation algorithm based on frequency domain analysis was implemented, aligning the smartphone coordinate system with actual walking direction through mathematical transformation rather than physical constraints. Additionally, the research examined WiFi positioning technology integration to mitigate cumulative errors inherent in standalone PDR systems.

The experimental design evaluated system performance under two prevalent smartphone carrying configurations (pocket mode and reading mode) while navigating predetermined trajectories incorporating multiple directional transitions. This methodological approach enabled comprehensive assessment of system adaptability across diverse usage contexts and its capacity to maintain localization precision throughout complex movement patterns.

5.2 Main Results

1. Step Detection Performance: The multi-sensor axis fusion methodology demonstrated robust gait detection capabilities across different smartphone carrying configurations. The optimal sensor axis arrangement (Accel_X-Accel_Y-Lin_Acc_Z) achieved nearly perfect step count accuracy in both tested carrying modes, identifying 89 steps in pocket mode and 92 steps in reading mode, precisely corresponding to actual step counts. This cross-sensor integration approach significantly outperformed conventional single-sensor methodologies and operated independently of smartphone orientation, constraining error margins within 3%, representing substantial improvement compared to the 10-20% error typically observed with traditional approaches.

2. Heading Estimation Performance: The posture-unconstrained heading estimation algorithm successfully captured directional transitions across both carrying configurations, albeit with varying degrees of precision. Average heading estimation deviation measured 22.74° in pocket mode, compared to 16.91° in reading mode. Although these values exceed ideal parameters, the system maintained sufficient accuracy for practical navigation applications, particularly considering the absence of orientation constraints and

other influential factors.

3. Trajectory Reconstruction: The PDR system exhibited differential trajectory reconstruction capabilities contingent upon carrying configuration. Pocket mode generated a terminal positioning deviation of 1.58 meters, while reading mode resulted in a substantially more pronounced displacement of 5.27 meters. This disparity underscores the susceptibility of heading estimation to hand movements in reading mode, which introduces systematic errors that propagate throughout the trajectory.

4. WiFi Integration Benefits: The incorporation of WiFi positioning technology with PDR substantially enhanced aggregate system effectiveness. The integration methodology reduced mean positioning error by approximately 37.5% in pocket mode (decreasing from 1.94 meters to 1.21 meters) and by 36.6% in reading mode (diminishing from 2.51 meters to 1.59 meters). The complementary filter-based fusion algorithm demonstrated consistent performance improvements across both carrying arrangements, validating its resilience across heterogeneous utilization contexts.

5.3 Conclusion

Several significant conclusions can be drawn from experimental findings and subsequent analysis:

1. Viability of Posture-Unconstrained Navigation: This investigation validates that effective pedestrian positioning can be accomplished without imposing rigid smartphone directional constraints through appropriate algorithmic implementations. By exploiting frequency domain properties and coordinate system transformations, the framework operates across conventional carrying arrangements without necessitating users to maintain predetermined device orientations.
2. Multi-Sensor Fusion Benefits: The exceptional efficacy of multi-sensor axis integration methodology in gait detection underscores the significance of considering individual sensor axes as discrete information channels rather than relying on aggregated signals from singular sensor categories. This approach successfully captures complementary locomotion characteristics across various dimensions, strengthening detection resilience and precision.
3. Imperative for Wireless Technology Integration: Despite enhancements in autonomous PDR algorithms, incorporating absolute positioning references (exemplified by WiFi) remains essential for longitudinal accuracy. The uniform error diminution observed across both carrying configurations demonstrates that sensor fusion effectively counteracts the progressive drift inherent in purely inertial navigation methodologies.

5.4 Research Limitations

There are several limitations that should be acknowledged in this study:

1. Environmental Constraints: Experiments were conducted within controlled corridor settings characterized by relatively uniform illumination, floor surfaces, and structural attributes. This configuration may insufficiently represent the heterogeneity and intricacy of authentic indoor environments, such as commercial centers, aviation terminals, or residential structures featuring diverse flooring materials, obstructions, and spatial arrangements.

2. Limitations of Stride Length Estimation: While the enhanced Weinberg model implemented in this study incorporates height characteristics and acceleration variations, it nevertheless represents a comparatively simplified approach to stride length estimation. The framework exhibits certain constraints when confronting varied walking velocities, terrain types (such as inclines or textured surfaces), and inter-individual biomechanical variations. Particularly during highly dynamic ambulation states (such as rapid walking or running) or under conditions of fatigue, the model may inadequately capture stride length variations. Furthermore, the static nature of model parameters results in limited real-time adaptive capability to sudden changes in locomotion state, potentially generating cumulative errors in specific scenarios.
3. Carrying Configuration Limitations: Although this investigation examined two prevalent smartphone carrying arrangements (pocket and reading modes), it did not explore additional frequently utilized scenarios, such as call positioning (device adjacent to ear), bag/purse placement, or specialized mounting configurations (arm straps, waist attachments). The system's efficacy across this broader spectrum of carrying methodologies necessitates additional examination.
4. Turn Detection Requirements: While the research framework acknowledges the significance of identifying and specifically addressing turning maneuvers, a comprehensive turn detection and processing mechanism has yet to be implemented and evaluated. Consequently, the current system's performance during complex movement patterns (abrupt directional changes, cessation of movement, retrograde locomotion) remains incompletely assessed.
5. Vertical Positioning Constraints: Although research objectives encompassed investigation of barometric sensing for altitude determination, this component has not been thoroughly developed or incorporated into the experimental framework. The present implementation remains confined to two-dimensional localization on a singular plane, leaving unaddressed the complexities associated with multi-level indoor navigation.

5.5 Future Research Plans

Based on research findings and identified limitations, several ideas for future directions :

1. Three-Dimensional Indoor Positioning: A natural extension of this work involves developing comprehensive three-dimensional indoor localization systems that incorporate vertical movement detection and floor identification capabilities. Future research should integrate barometric sensing to detect elevation changes and develop algorithms capable of accurately recognizing floor transitions during stair climbing, elevator utilization, or escalator traversal.
2. Advanced motion Pattern Recognition: Developing specialized detection frameworks for identifying complex movement patterns represents a crucial future research trajectory. This encompasses automated recognition of directional changes, stairway navigation, elevator transport, escalator utilization, and stationary intervals. Machine learning methodologies, particularly deep learning architectures trained on annotated Inertial Measurement Unit (IMU) datasets, could facilitate classification of these mobility categories, enabling tailored processing for individual scenarios and enhancing localization precision during transitional movement phases.

3. Enhanced Heading Estimation: Further refinement of frequency domain heading estimation techniques is essential to minimize observed directional deviations. Subsequent research should investigate wavelet transformation as an alternative to Fourier analysis for superior characterization of non-stationary signal properties during pedestrian locomotion. Additionally, dynamic parameter optimization frameworks could automatically recalibrate filtration variables according to identified movement conditions.

4. Expanded Fusion Architecture: Extending the sensor integration framework to incorporate supplementary localization technologies such as Bluetooth Low Energy beacons, ultrasonic distance measurement, or visual-inertial odometry would further enhance system resilience. Factor graph optimization methodologies could efficiently consolidate these heterogeneous information sources with appropriate uncertainty modeling constructs.

BIBLIOGRAPHY

[1] N. Klepeis, W. Nelson, W. Ott *et al.*, "The National Human Activity Pattern Survey (NHAPS): a resource for assessing exposure to environmental pollutants," *Journal of Exposure Science and Environmental Epidemiology*, vol. 11, pp. 231–252, 2001.

[2] P. Bellavista, A. Kupper, and S. Helal, "Location-based services: Back to the future," *IEEE Pervasive Computing*, vol. 7, no. 2, pp. 85–89, 2008.

[3] B. Rao and L. Minakakis, "Evolution of mobile location-based services," *Communications of the ACM*, vol. 46, pp. 61–65, 2003.

[4] A. El-Rabbany, "Introduction to gps: The global positioning system," *Satellite Navigation Systems*, 2006.

[5] H. Liu, H. Darabi, P. Banerjee, and J. Liu, "Survey of wireless indoor positioning techniques and systems," *IEEE Transactions on Systems, Man, and Cybernetics, Part C (Applications and Reviews)*, vol. 37, no. 6, pp. 1067–1080, 2007.

[6] M. Youssef, "The horus wlan location determination system," in *Proceeding of International Conference on Mobile Systems, Applications, and Services*, 2005, pp. 357–374.

[7] L. Chen, L. Pei, H. Kuusniemi *et al.*, "Bayesian fusion for indoor positioning using bluetooth fingerprints," *Wireless Personal Communications*, vol. 70, no. 4, pp. 1735–1745, 2013.

[8] M. Hazas and A. Hopper, "Broadband ultrasonic location systems for improved indoor positioning," *IEEE Transactions on Mobile Computing*, vol. 5, no. 5, pp. 536–547, 2006.

[9] R. Harle, "A survey of indoor inertial positioning systems for pedestrians," *IEEE Communications Surveys & Tutorials*, vol. 15, no. 3, pp. 1281–1293, 2013.

[10] J. Kang, J. Lee, and D. S. Eom, "Smartphone-based traveled distance estimation using individual walking patterns for indoor localization," *Sensors*, vol. 18, no. 9, pp. 1385–1396, 2018.

[11] J. Qian, J. Ma, R. Ying *et al.*, "An improved indoor localization method using smartphone inertial sensors," in *International Conference on Indoor Positioning and Indoor Navigation*, Montbeliard, 2013.

[12] F. Laricchia, "Smartphones - statistics and facts," 2024, available at https://www.statista.com/topics/840/smartphones/, accessed on 2024-03-04.

[13] M. Susi, V. Renaudin, and G. Lachapelle, "Motion mode recognition and step detection algorithms for mobile phone users," *Sensors*, vol. 13, pp. 1539–1562, 2013.

[14] D. Liu, L. Pei, J. Qian, L. Wang, P. Liu, Z. Dong, S. Xie, and W. Wei, "A novel heading estimation algorithm for pedestrian using a smartphone without attitude constraints," in *2016 Fourth International Conference on Ubiquitous Positioning, Indoor Navigation and Location Based Services (UPINLBS)*, 2016, pp. 29–37.

[15] A. Correa, M. Barcelo, A. Morell, and J. L. Vicario, "A review of pedestrian indoor positioning systems for mass market applications," *Sensors*, vol. 17, no. 8, p. 1927, 2017.

[16] C. Isaia and M. P. Michaelides, "Step counting by optimum fusion of imu sensor measurements," in *Proceedings of the Work-in-Progress Papers at the 14th International Conference on Indoor Positioning and Indoor Navigation*, ser. IPIN-WiP 2024, 2024, pp. 1–9. [Online]. Available: https://github.com/conisaia/Step-Counting-by-Optimum-Fusion-of-IMU-Sensor-Measurements

[17] L.-H. Chen, E. H.-K. Wu, M.-H. Jin, and G.-H. Chen, "Intelligent fusion of Wi-Fi and inertial sensor-based positioning systems for indoor pedestrian navigation," *IEEE Sensors Journal*, vol. 14, no. 11, pp. 4034–4042, 2014.

[18] X. Kang, B. Huang, and G. Qi, "A novel walking detection and step counting algorithm using unconstrained smartphones," *Sensors*, vol. 18, no. 1, 2018. [Online]. Available: https://www.mdpi.com/1424-8220/18/1/297

[19] M.-S. Pan and H.-W. Lin, "A step counting algorithm for smartphone users: Design and implementation," *IEEE Sensors Journal*, vol. 15, no. 4, pp. 2296–2305, 2015.

[20] F. Gu, K. Khoshelham, J. Shang, F. Yu, and Z. Wei, "Robust and accurate smartphone-based step counting for indoor localization," *IEEE Sensors Journal*, vol. 17, no. 11, pp. 3453–3460, 2017.

[21] D. Salvi, C. Velardo, J. Brynes, and L. Tarassenko, "An optimised algorithm for accurate steps counting from smart-phone accelerometry," in *2018 40th Annual International Conference of the IEEE Engineering in Medicine and Biology Society (EMBC)*, 2018, pp. 4423–4427.

[22] G. Zhao, X. Wang, H. Zhao, and Z. Jiang, "An improved pedestrian dead reckoning algorithm based on smartphone built-in mems sensors," *AEU - International Journal of Electronics and Communications*, vol. 168, p. 154674, 2023. [Online]. Available: https://doi.org/10.1016/j.aeue.2023.154674

[23] J. Kuang, X. Niu, and X. Chen, "Robust pedestrian dead reckoning based on mems-imu for smartphones," *Sensors*, vol. 18, no. 5, 2018. [Online]. Available: https://www.mdpi.com/1424-8220/18/5/1391

[24] J. Geng, L. Xia, J. Xia, Q. Li, H. Zhu, and Y. Cai, "Smartphone-based pedestrian dead reckoning for 3d indoor positioning," *Sensors*, vol. 21, no. 24, 2021.

[25] G. Wang, X. Wang, J. Nie, and L. Lin, "Magnetic-based indoor localization using smartphone via a fusion algorithm," *IEEE Sensors Journal*, vol. 19, no. 15, pp. 6477–6485, 2019.

[26] Z. Tian, Y. Zhang, M. Zhou, and Y. Liu, "Pedestrian dead reckoning for marg navigation using a smartphone," *EURASIP Journal on Advances in Signal Processing*, vol. 2014, p. 65, 2014.

[27] W. Kang and Y. Han, "Smartpdr: Smartphone-based pedestrian dead reckoning for indoor localization," *IEEE Sensors Journal*, vol. 15, no. 5, pp. 2906–2916, 2015.

[28] M. Vezočnik, R. Kamnik, and M. B. Juric, "Inertial sensor-based step length estimation model by means of principal component analysis," *Sensors*, vol. 21, no. 10, p. 3527, 2021.

[29] B. Khalili, R. Ali Abbaspour, A. Chehreghan, and N. Vesali, "A context-aware smartphone-based 3d indoor positioning using pedestrian dead reckoning," *Sensors*, vol. 22, no. 24, p. 9968, 2022. [Online]. Available: https://doi.org/10.3390/s22249968

[30] H. Zhao, W. Cheng, N. Yang, S. Qiu, Z. Wang, and J. Wang, "Smartphone-based 3d indoor pedestrian positioning through multi-modal data fusion," *Sensors*, vol. 19, no. 20, 2019. [Online]. Available: https://www.mdpi.com/1424-8220/19/20/4554

[31] H. Zhou and T. Maekawa, "Gps-assisted indoor pedestrian dead reckoning," *Proceedings of the ACM on Interactive, Mobile, Wearable and Ubiquitous Technologies*, vol. 6, no. 4, 2023.

[32] G. Chandra, "Position estimation at indoors using wi-fi and magnetic field sensors," in *IPIN-WiP*, 2022.

[33] I. Ashraf, S. Hur, and Y. Park, "Enhancing performance of magnetic field based indoor localization using magnetic patterns from multiple smartphones," *Sensors*, vol. 20, no. 9, 2020. [Online]. Available: https://www.mdpi.com/1424-8220/20/9/2704

[34] S. Soheil and T. Federico, "A survey on the computation of quaternions from rotation matrices," *Journal of Mechanisms and Robotics*, 2019.

[35] R. G. Valenti, I. Dryanovski, and J. Xiao, "Keeping a good attitude: A quaternion-based orientation filter for IMUs and MARGs," *Sensors*, vol. 15, no. 8, pp. 19 302–19 330, 2015.

[36] S. Bai, W. Wen, Y. Li, C. Shi, and L.-T. Hsu, "Toward persistent spatial awareness: A review of pedestrian dead reckoning-centric indoor positioning with smartphones," *IEEE Transactions on Instrumentation and Measurement*, vol. 73, pp. 1–28, 2024.

[37] H. Weinberg, "Using the adxl202 in pedometer and personal navigation applications," *Analog Devices Application Note AN-602*, 2002.

[38] N.-H. Ho, P. H. Truong, and G.-M. Jeong, "Step-detection and adaptive step-length estimation for pedestrian dead-reckoning at various walking speeds using a smartphone," *Sensors*, vol. 16, no. 9, p. 1423, 2016.

[39] A. E. Cetin, O. N. Gerek, and Y. Yardimci, "Equiripple FIR filter design by the FFT algorithm," *IEEE Signal Processing Magazine*, vol. 14, no. 2, pp. 60–64, 1997.

[40] V. Renaudin, M. H. Afzal, and G. Lachapelle, "Magnetic perturbations detection and heading estimation using magnetometers," *Journal of Location Based Services*, vol. 6, no. 3, pp. 161–185, 2012.

[41] J. Qian, L. Pei, D. Zou *et al.*, "Optical flow-based gait modeling algorithm for pedestrian navigation using smartphone sensors," *IEEE Sensors Journal*, vol. 15, no. 12, pp. 6797–6804, 2015.

[42] H. Zhou, D. Zou, L. Pei *et al.*, "StructSLAM: Visual SLAM with building structure lines," *IEEE Transactions on Vehicular Technology*, vol. 64, no. 4, pp. 1364–1375, 2015.

[43] D. Liu, L. Pei, J. Qian *et al.*, "Simplified ellipsoid fitting-based magnetometer calibration for pedestrian dead reckoning," in *China Satellite Navigation Conference (CSNC) 2016 Proceedings*, vol. II. Springer Singapore, 2016, pp. 473–486.

APPENDICES

APPENDIX I

Title of Appendix

If you have material that cannot be included within your document, you must include an appendix. You may include one appendix or a number of appendices. If you have more than one appendix, you would number each accordingly (i.e., Appendix I, Appendix II, etc.). Write your appendix headings in the same manner as your chapter headings.